Analysis fire patterns and drivers with a global SEVER-FIRE v1.0 model incorporated into Dynamic Global Vegetation Model and satellite and on-ground observations.

Sergey Venevsky[1], Y. Le Page[2], J.M.C. Pereira[2], Chao Wu[1]

1 Ministry of Education Key Laboratory for Earth System Modeling, Department of Earth System Science, Tsinghua University, Beijing 100084, China

2 Technical University of Lisbon, Instituto Superior de Agronomia, Department of Forestry, Tapada da Ajuda 1349-017 Lisboa, Portugal

Correspondence to: Chao Wu(wuc14@mails.tsinghua.edu.cn) and Sergey Venevsky (venevsky@tsinghua.edu.cn)

Abstract. Biomass burning is an important environmental process with a strong influence on vegetation and on the atmospheric composition. It competes with microbes and herbivores to convert biomass to CO_2 and it is a major contributor of gases and aerosols to the atmosphere. To better understand and predict global fire occurrence, fire models have been developed and coupled to Dynamic Global Vegetation Models (DGVMs) and Earth System Models (ESMs).

We present SEVER-FIRE v1.0 (Socio-Economic and natural Vegetation ExpeRimental global fire model version 1.0) which is incorporated into the SEVER-DGVM. One of the major focuses of SEVER-FIRE model is an implementation of pyrogenic behaviour of humans (timing of their activities and their willingness/necessity to ignite or suppress fire), related to socio-economic and demographic conditions in a geographical domain of the model application. Burned areas and emissions from the SEVER model are compared to the Global Fire Emission Database version 2 (GFED), derived from satellite observations, while number of fires are compared with regional historical fire statistics. We focus both on the model output accuracy and on its assumptions regarding fire drivers, and perform:

1- An evaluation of the predicted spatial and temporal patterns, focusing on fire incidence, seasonality and inter-annual variability.

2- Analysis to evaluate the assumptions concerning the etiology, or causation, of fire, including climatic and anthropogenic drivers, as well as the type and amount of vegetation.

SEVER reproduces the main features of climate driven inter-annual fire variability at a regional scale, such as the large fires associated with the 1997-98 El Niño event in Indonesia, Central and South America, which had critical ecological and atmospheric impacts. Spatial and seasonal patterns of fire incidence reveal some model inaccuracies, and we discuss the implications of the distribution of vegetation types inferred by the DGVM, and of assumed proxies of human fire practices. We further suggest possible development directions, to enable such models to better project future fire activity.

1 Introduction

The biosphere is affected by fires through physical and chemical pathways, involving interactions between the terrestrial and atmospheric components of carbon, water and nutrients cycles. As a natural phenomenon, fires are an integral part of a majority of ecosystems, influencing soil fertility, stand regeneration, vegetation composition, and succession (Le Page et al., 2015; Levine et al., 1999). However, through its anthropogenic use for land management (agriculture, pasture, deforestation), fire incidence is considerably higher than under natural conditions in many regions, including savannas in Africa and Australia, or tropical forests in South America and South East Asia (Bond et al., 2005).

Abundant literature points a variety of impacts, roles, and drivers of fires, and an extended range of spatial and time scales involved. It is estimated that, on average, an area equivalent to that of India burns every year, predominantly in savannas and grasslands (Tansey et al., 2004). Burned areas in tropical and boreal forests are smaller, but their high productivity and carbon storage capacity results in significant emissions of numerous greenhouse gases (e.g. CO_2, CH_4 (Andreae and Merlet, 2001; Pereira et al., 1999)). Globally, total fire emissions are equivalent to approximately one third of fossil fuel burning emissions (Le Quéré et al., 2015; van der Werf et al., 2006; Wu et al., 2017). Net emissions, stemming from deforestation or increased fire activity, are much smaller, but poorly constrained (van der Werf et al., 2006), and highly variable on inter-annual time scales, especially through induced changes in fire sensitivity of highly productive ecosystems by El Niño/La Niña and other climatic phenomena (Duncan et al., 2003; Langenfelds et al., 2002; Le Page et al., 2008; van der Werf et al., 2004; van der Werf et al., 2008).

The strong integration of fires with the biosphere system is also emphasized by their dependence on a complex system of interactive drivers, designated as the fire triangle (Schoennagel et al., 2004), dominated by climate, vegetation and human activities. Precipitation rates and temperature partly control the amount of fuel available to burn, its moisture content, and fire behaviour in case of ignition (Crevoisier et al., 2007; Turner et al., 2008). Fire incidence, fire severity, and ensuing emissions are also dependent on the vegetation types, structure and productivity of the ecosystem (Andreae and Merlet, 2001; Hammill and Bradstock, 2006). Finally, anthropogenic activities, as mentioned above, greatly bias the natural occurrence of fires, increased in many regions as a land management tool, or decreased through fire

suppression strategies (firefighting, preventive fires (Veblen et al., 2000)). Other factors are involved (topography, natural landscape breaks, grazing), but most important is the interaction between those drivers, which needs to be considered to yield relevant information about fire risk (Dwyer et al., 2000a).

Dynamic Global Vegetation Models (DGVMs) and Earth System Models (ESMs) simulate vegetation dynamics at global scale, fire is included as an explicit process in some of these models (Arora and Boer, 2005; Bachelet et al., 2001; Li et al., 2013; Rabin et al., 2018; Thonicke et al., 2010; Thonicke et al., 2001; Venevsky et al., 2002; Wu et al., 2017; Yue et al., 2014). Given the importance of fires and their dependence on various model inputs or simulated processes, the development of fire modules is of great interest to understand and evaluate the fire related couplings and feedbacks assumptions. Comprehensive review of global fire modelling activity is given by Hantson et al. (2016) and an overview of recent global fire models participating in the Fire Modelling Intercomparison Project (FireMIP) is presented by Rabin et al. (2017). Hantson et al. (2016) distinguish four level of complexity for global fire models incorporated into DGVMs (see Figure 2 in their study) depending on processes included in models:

1) Simplest statistical model relates areas burnt with climate and/or vegetation (Glob-FIRM (Thonicke et al., 2001)) and/or human activities (Knorr et al., 2014).
2) Models estimating statistically number of fires and expected size of fires (Pechony and Shindell, 2009).
3) Process-based quasi-mechanistic models which use functional relationships between climate, vegetation and socio-economic drivers of wildfires (MC-FIRE (Lenihan and Bachelet, 2015), CTEM (Arora and Boer, 2005), CLM-Li (Li et al., 2013), LM3-FINAL (Rabin et al., 2018) etc.). This approach was firstly introduced by Reg-FIRM model (Venevsky et al., 2002) and further developed by follow-up SPITFIRE (Thonicke et al., 2010) model and is derivatives (JSBACH-SPITFIRE (Lasslop et al., 2014), LPJ-LMfire (Pfeiffer et al., 2013), LPJ-GUESS-SPITFIRE (Lehsten et al., 2009), ORCHIDEE-SPITFIRE (Yue et al., 2014), and LPX-Mv1 (Kelley and Harrison, 2014).
4) Complete representation of all processes in space and time (first-principle approach model).

Nine from the 11 global models participating in FireMIP experiment are process-oriented quasi-mechanistic models (Rabin et al., 2017), however, mainly due to complexity of the processes involved all these models are still not at the level 4. The closest to the complete representation of all fire related processes in time is SPITFIRE model (see Table 1 in Hantson et al. (2016)) and their modifications. SPITFIRE modelling community achieved significant results in global and regional fire modelling describing dynamics of wildfires in savannah – forest transition zone (Baudena et al., 2015),

contemporary dynamics of areas burnt in Europe (Wu et al., 2015), global fire regimes in pre-industrial zone (Pfeiffer et al., 2013) and changes in global carbon balance (Prentice et al., 2011).

While complete representation of all processes which determine wildfire dynamics in space and time is still under its way, quasi-mechanistic models use different parametrisations of ignitions and spread of wildfire. Parametrisations are based either on long term fires statistics, or on remote sensing data which are valuable data source due to its availability and global coverage. SPITFIRE model, for example, use lightning frequency as an input for calculation of number of lightning fires. We argue that it would be advantageous if one can produce long-term fire relationships without depending on remote-sensing, which is available for a relatively short period of time (a few decades). Fire return intervals can be of the order of hundreds of years, whereas remote sensing is available for several decades. Therefore, using remote sensing to derive relationships implicitly assumes a space for time substitution, which may or may not hold. On the other hand, parameterisations based on ground-based measurements or laboratory-based experiments have their own problems, like insufficient accuracy and low representativeness in space, but considered to be more robust in time and, thus, very useful in DGVMs or ESMs for investigation of future global change impacts or past global fire regimes reconstruction.

We present in this study SEVER-FIRE v1.0 (Socio-Economic and natural Vegetation ExpeRimental global fire model version 1.0; simplified as SEVER-FIRE in the following text) incorporated into the SEVER-DGVM (Venevsky and Maksyutov, 2007; Wu et al., 2017), which is a modification of LPJ-DGVM (Sitch et al., 2003) for daily time step computation. SEVER-FIRE is a quasi-mechanistic model, which is a follow up of Reg-FIRM for the globe, with several new features aiming approaching to complete representation of wildfire processes. We improve earlier algorithms of Reg-FIRM and introduce new functionality with respect: 1) to estimate the numbers of lightning fires from data on convective activity in the atmosphere 2) to estimate numbers of human fires from urban against rural population (timing of their appearance in natural landscapes and their ratio) and regional wealth index, as well 3) to estimate more realistically fire duration, which in the new model depends on human suppression and weather situation and can last for up to two days. One of the major focuses of SEVER-FIRE model is an implementation of pyrogenic behaviour of humans (timing of their activities and their willingness/necessity to ignite or suppress fire), related to socio-economic and demographic conditions in a geographical domain of the model application. Importance of description of pyrogenic behaviour of humans are confirmed by recent findings of bi-modal fire regimes, reflecting human fingerprint in global fires dynamics (Benali et al., 2017), as well as by differences in timing of ignitions determined by religious background in Sub-Sahara Africa (Pereira et al., 2015). Fire weather regimes, set by climate dynamics, and fuel state set by vegetation dynamics are other important drivers in SEVER-FIRE model. SEVER-DGVM fire module, based on climate observations, external anthropogenic parameters, and

SEVER-DGVM derived vegetation, estimates fire incidence and emissions. The resulting vegetation disturbance feeds back to the DGVM, ensuring a fully coupled system (see model description).

We perform a comparison of SEVER outputs with fire data derived from satellite sources, the Global Fire Emission Database version 2 (GFED) (van der Werf et al., 2006), as well as with historic fire data (number of lightning and human fires and their area burnt) with two objectives. First, a global evaluation of a DGVM-fire model, focusing on crucial and simple features, namely fire incidence, seasonality, inter-annual variability, and emissions. Second, (the most important) by identifying the reasons for large inconsistencies we propose further modifications to SEVER-FIRE. The work presented in this paper is partly based on the Ph.D. thesis by Y. Le Page. We therefore signal the reader that significant parts of the text in the sections 3 and 4 already appeared in Le Page (2009).

We are making an effort to make a closer step to a first-principle global mechanistic fire model. We have named our model 'Experimental' in order to show that some processes are included in SEVER-FIRE model ad hoc (timing of ignition activity of rural versus urban population, others) as mechanisms are still not described/studied, some processes are simplified (e.g., setting maximum time of fire to two days but this may be updated and modified in the future by introducing the latest global fire duration datasets (Andela et al., 2018)) and some processes are based on statistical descriptions from satellite data (number of on-ground flashes), as they wait there nearest time to be substituted by physically based mechanistic models.

2. Data and Methods

2.1 SEVER-DGVM and SEVER-FIRE Models

2.1.1 Input of DGVM to fire model

SEVER-DGVM is a coupled vegetation-fire mechanistic model designed to run at a range of temporal (daily to monthly) and spatial (10 km to 2.5 º with 0.5º mostly tested) resolution levels (Venevsky and Maksyutov, 2007). The fire module SEVER-FIRE is a further development of the Reg-FIRM (Venevsky et al., 2002), which was applied only for Iberian Peninsula, from a regional to the global scale. The aim of this model is to provide at the global scale a comprehensive mechanistic description of major characteristics registered in standard fires statistics and/or satellite observations around the world, namely number of fires, area burnt and carbon emissions. An important goal of SEVER-FIRE model is inclusion in Earth System models (Bonan and Doney, 2018; Bowman et al., 2009) in order to make realistic climate change predictions of global wildfire dynamics. The most important variables, provided by SEVER-DGVM for SEVER-FIRE model include the distribution of 10 Plant Functional Types (PFTs) , which are similar to LPJ-DGVM vegetation types (see names of PFT in Table 1) over the globe, described as a

distribution of fractions within a grid cell $Cveg_{pft}$, net primary productivity NPP_{pft}, carbon of aboveground vegetation c_{pft}, fuel loading lit_{pft}, described as a mass of litter, and soil moisture $moist$ in the upper 0.1 m layer m (see Table 1 for description of fire model variables and parameters)

2.1.2 External input to fire model

Gridded climate, demographic and socio-economic data comprise external input for the fire module. Minimum/maximum daily temperature $t_{min/max}$, daily precipitation/convective precipitation $prec/cprec$ and wind speed u are the climate variables used in SEVER-FIRE. Human population density P, ratio of rural to total population (rural and urban population) $rur = \frac{P_{rur}}{P_{tot}}$, wealth index WI and average distance from megacities $dist$ (recalculated with simplified assumptions from population density and ratio of rural to urban population) comprise socio-economic input to the fire model.

2.1.3 Output of fire model

The model separates human-induced (indexed as *hum*) and lightning fires (indexed as *nat*) by sources of ignition and all output variables of fire models can be obtained either by these two classes of fires of for both classes in total as their sum (not indexed). We omit the mentioned indexes in description of output variables further on for simplicity. The output of the model includes number of fires $Nfire$, area burnt $aburnt$, fire carbon emission $cfire$, number of PFT's individuals killed $Nind_{pft}$ and updated vegetation carbon and NPP. Fire model feedbacks to the DGVM through the increased area (equal to burnt areas by PFTs) and decreased number of PFT's individuals for competitive occupation by PFTs after a fire and updated carbon fluxes and pools for carbon cycle simulation within vegetation model.

Thus, the DGVM and fire module work in interactive mode, incorporating a representation of fire-vegetation feedbacks.

2.1.4 Components of SEVER-FIRE

The SEVER-FIRE model consists of six related components described below:

- Estimation of fire weather danger index and fire probability,
- Simulation of lightning ignition events and number of lightning fires,
- Simulation of human ignition events and number of human fires,
- Simulation of fire spread after ignition,
- Fire termination,

- Estimation of fire effects (areas burnt, pyrogenic emissions, number of each PFT individuals killed).

All six components are controlled by PFT dependent fire parameters (see list in Table 1)

1) Estimation of fire weather danger index and fire probability

Fire weather danger index *FDI(d)*, measured from 0 ("no fire danger"), to 1 ("extreme fire danger"), is estimated in SEVER-FIRE based on the Reg-FIRM fire danger index (Venevsky et al., 2002). It is calculated at a daily time step as a multiple of exponentially normalized Nesterov Index (based on accumulated difference of minimum and maximum temperature, forced to zero by 3 mm daily precipitation threshold) and vegetation and soil moisture dependent fire probability. Using of Reg-FIRM based fire weather danger indexes, became popular in contemporary global fire modelling (Arora and Boer, 2005; Thonicke et al., 2010) mainly due to calculation simplicity. Direct comparison of fire risk for Siberia, described by more sophisticated Canadian Fire Danger and Russian Fire Danger Indexes (used by national Forest Service) in both countries with Reg-FIRM Fire Danger Index, revealed that they are almost equivalent (Rubtsov, personal communication). The fire probability function is designed as a regression from observations (Thonicke et al., 2001). It depends on current soil moisture in the upper 10 cm layer and PFT dependent fire moisture of extinction (Table 1), adapted from experimental study of Albini (1976).

2) Simulation of lightning ignition events and number of lightning fires

The number of potential lightning ignitions in a grid cell is calculated from the daily number of cloud-to-ground flashes $N_{flashes}$, which is estimated from convective precipitation as a non-linear regression polynomial function of power four (as in Allen and Pickering (2002)). Using of power four polynomial function by convective precipitation to represent number of flashes has theoretical physical grounds (Vonnegut, 1963). Allen and Pickering (2002) prepared their parametrization of number of flashes for North America, so we made a validation test of $N_{flashes}$ for the globe (Venevsky, 2014) using OTD-LIS observed lightning data (Christian Hugh et al., 2003) and found that the parametrization performs well at global scale (R^2=0.51). Cloud-to-ground flashes are divided to negatively charged (90%) and positively charged (10%) (Latham and Schlieter, 1989). Only the flashes with long continuous current (LCC flashes, 75% of positively charged and 25% of negatively charged) can ignite wildfire (Latham and Schlieter, 1989). Efficiency of LCC flashes to ignite depends from bulk density of fuel as it was shown in laboratory (Latham and Schlieter, 1989), so number of efficient to ignite positive flashes ${N_{flashes}}_{pos}^{eff}$ and number of efficient to ignite negative flashes ${N_{flashes}}_{neg}^{eff}$ at first glance can be simplified as Eq. (1) and Eq. (2):

$$N_{flashes}{}_{pos}^{eff} = N_{flashes} * 0.1 * 0.75 * b * a * dens * \bar{t}_{thunder}, \quad (1)$$

$$N_{flashes}{}_{neg}^{eff} = N_{flashes} * 0.9 * 0.25 * b * a * dens * \bar{t}_{thunder}, \quad (2)$$

where b =0.1 is efficiency of lightning *t* ignite (Latham and Schlieter, 1989), a=0.25 m^2/kgC regression coefficient (simplified from Latham and Schlieter (1989)), $\bar{t}_{thunder}$ is an average daily time of thunder over a grid cell, set to one hour and twenty minutes (Uman, 1987) and *dens* is bulk density of fuel (kgC/m^2). Bulk density of fuel is an important variable of SEVER-FIRE model, used in several basic equations. We assume that all PFTs found in a grid cell are distributed homogeneously and bulk density of fuel in a grid cell is calculated as Eq. (3):

$$dens = \sum_{i=1}^{Npft} Cveg_{PFT}(i) * dens_{PFT}(i), \quad (3)$$

where $Cveg_{PFT}(i)$ is foliar projection cover of *i*-th PFT, $dens_{PFT}(i)$ is bulk density of *i*-th PFT (see Table 1), which are taken from Reg-FIRM (Venevsky et al., 2002) and study of Albini (1976), $Npft$ is total number of PFTs in a grid cell. Bulk density of fuel in the grid cell and depth of fuel (in cm), calculated as Eq. (4):

$$depth = 0.1 * \sum_{i=1}^{Npft} lit_{PFT}(i) / dens, \quad (4)$$

and they are translated into arriving daily number of natural ignitions from positive $N_{ignitions}{}_{pos}$ and negative flashes $N_{ignitions}{}_{neg}$, using fitting into two functions of data for probability to ignite for positive and negative flashes by eight fuel types (see Table 1 of Anderson (2002)), obtained from laboratory experiments (Eq. (5) and (6)):

$$N_{ignitions}{}_{pos} = (1/(1 + \exp(5.5 * (1./1.5) ** (((16. - dens)/16.) * 5) * 1.25 - 1.2 * 0.5 ** ((16. - dens)/16.* 5. + 0.1) * depth))) * N_{flashes}{}_{pos}^{eff}, \quad (5)$$

$$N_{ignitions}{}_{neg} = (1/(1 + \exp(5.5 * (1./1.5) ** (((16. - dens)/16.) * 5) - 1.2 * 0.5 ** ((16. - dens)/16.* 5.) * depth))) * N_{flashes}{}_{neg}^{eff}. \quad (6)$$

Total number of arriving ignitions from effective positive and negative LCC flashes are recalculated into number of surviving natural fires $N_{fires}{}_{nat}$ in a grid cell with area S_{grid}, which depends on daily fire danger index $FDI\ (d)$ maximum rate of surviving ignitions $rate_{survival}{}_{max}$, taken as 0.15 (Anderson,

2002) and soil moisture in 1 cm fuel layer, simplified as 10% of soil moisture *moist* in upper 10 cm, see Eq. (7):

$$N_{fires_{nat}}(d) = FDI\ (d) * (N_{ignitions_{pos}} + N_{ignitions_{neg}}) * rate_{survival_{max}} * (1 - moist * 0.1) * 0.15 * (1 + 0.0001 * (elev - 1000))^4 * S_{grid}. \quad (7)$$

Dependence of number of lightning fires in Eq. (7) by elevation $elev$ in meters was obtained by linear regression from data of Vazquez and Moreno (1998) for Peninsular Spain. Module of number of lightning fires was validated using data for lightning and lightning fires in central cordillera of Canada (Wierzchowski et al., 2002). This study contains data for number of lightning fires for the years 1961-1994 and annual number of lightning strikes for 1989-1994 for the central cordillera area 50-54°N, 114-120°W. The central mountain range in the area divides it into two parts, one is in British Columbia, another in Alberta provinces. SEVER-FIRE is able to reproduce values for total annual number of lightning strikes for both provinces (see Fig. 1) and number of lightning fires in the provinces (see Fig. 2).

The model reproduces three to two fold dominance of annual number of lightning strikes in Alberta and seven to ten fold dominance of annual number of lightning fires in British Columbia. Using of convective precipitation as a driver for number of lightning fires also confirmed by study of Cardoso Manoel et al. (2007), who found that lightning fire occurrence in Brazil is related to zonal flux of moisture in the atmosphere.

3) Simulation of human ignition events and number of human fires

The number of potential human ignitions $N_{ignitions\_human}(d)$ is calculated as a power function from population density with saturation, suggested by the Russian Forest Service and also used in the Reg-FIRM (Venevsky et al., 2002) multiplied by normalized socio-economic characteristics of population and by fuel conditions (see Eq. (8)):

$$(N_{ignitions\_human_j}(d) = 6.8 * P^{0.43} * \bar{a} * rate_{pop_j} * timing_j(d) * a * dens, \quad (8)$$

where P is population density in persons per km^2, $\bar{a}$ is a mathematical expectation of number of ignition produced by one person for one million hectares, a= 0.125*10^{-4} [km^2/million hectares * m^2/kgC] (scaling coefficient from million hectares to square kilometers (Venevsky et al., 2002), divided by average fuel density 8 kgC/m^2) j is either rural (j=*rur*) or urban population (j=*urb*), $rate\_pop_j$ is a ratio of rural to total population, so that $rate\_pop_{rur} + rate\_pop_{urb} = 1$, $timing_j(d)$ is daily timing of pyrogenic activity of population. Timing of human pyrogenic activity $timing_j(d)$ at a first glance is defined

separately for the northern and southern hemisphere and for rural and urban population as a step function, and it is mostly based on agricultural and vacation calendars (for city inhabitants). It is set so that sum of $timing_{rural}(d)$ and $timing_{urban}(d)$ is equal always to one. So, for example, for the entire northern hemisphere it was set to one in July, August (Summer vacations) for urban population (zero for rural population in these months), March, April, May (Spring agriculture activities) and September, October, November (Autumn agriculture activities) for rural population (zero for urban population in these months) and to 0.5 in the rest of a year.

Mathematical expectation of number of ignition produced by one person for one million hectares $\bar{a}$ is set to be an exponential function of wealth index WI, determined from the data of UN Human Settlemnet Program (see Eq. (9)):

$$\bar{a} = \exp(-7.65 * 10^{-2} * WI). \quad (9)$$

Equation (9) was obtained using logarithmic regression from geographically distributed observed number of human fires (map of average over 1974-1994 annual number of human fires for Spain (Vazquez and Moreno, 1998), map of average over annual number of human fires by Canadian ecoregions 1961-1995 (Stocks et al., 2002) and map of average over annual number of total fires (assumed to be all human) by African countries 1981-1991 (Barbosa et al., 1999b). No division to rural and urban population was assumed when deriving Eq. (9). Equation (9) assumes that maximum mathematical expectation of number of ignition produced by one person is equal to one million hectares for a day (estimate of Russian Forest Service, see Melekhov (1978)), for a grid cell with the most theoretically possible poorest population (WI=0) and $\bar{a}$ =0.1 ignition/day*person*million hectares for a grid cell with the most theoretically wealthy population (WI=30 – closest is the Stockholm metropolitan area). Average value of $\bar{a}$ is equal to 0.22 ignition/person*million hectares (WI=20.5) for peninsular Spain as in Reg-FIRM (Venevsky et al., 2002).

Total number of human fires in a grid cell is calculated as Eq. (10):

$$N_{fires_{hum}}(d) = FDI\,(d) * (N_{ignitions\_hum_{rur}} + N_{ignitions_{urb}}) * S_{grid} \quad (10)$$

The number of human fires for peninsular Spain was validated for Reg-FIRM, which has the same equations as SEVER-FIRE in the region. To check plausibility of approach for calculation of total number of fires, we make validation for Canada for 1961-1995 (Stocks et al., 2002) (see Fig. 3), because Canada has significant variation for climatic conditions, vegetation composition, population density and socio-economic state of population.

The description of human ignitions in SEVER-FIRE model is very simplistic and does not have intention to describe to major extent complex economic, cultural and social practice of people (agricultural, hunting or pastoral, other) resulting in pyrogenic activities. We left out (or oversimplified, like in the timing function and mathematical expectation of number of ignition produced by one person) description of an influence of land use to number of human ignitions in the fire model, because SEVER-DGVM anyway does not include description of human land use and/or its influence to natural vegetation. By application of SEVER-DGVM we aim to describe relatively human-less global vegetation, which got additional control regulator, namely external human and/or lightning ignitions. This limitation of SEVER-DGVM implies certain constraints on our results in both vegetation distribution and areas burnt, but it also gives us an opportunity to identify and locate the areas, where interaction between land use, fire regimes and vegetation should be described explicitly and accurately.

4) Simulation of fire spread after ignition

Rate of fire spread after an ignition event is simulated using a simplified version of the Rothermel thermodynamic equation (Venevsky et al., 2002), and depends on wind speed, fuel bulk density and soil moisture content in the upper layer as a proxy of fuel moisture. As in the Reg-FIRM approach, a fire cannot take place when fuel loading threshold (100 g/m^2), calculated as litter pool by a DGVM, is not crossed. Simulation of rate spread, using Rothermel equation, in SEVER-FIRE is similar to the one used by some of recent landscape fire models (Cary et al., 2006) and other global fire models (Li et al., 2013; Rabin et al., 2017; Yue et al., 2014). However, there is a large difference in translation of rate of fire spread into areas burnt in landscape models and SEVER-FIRE. Indeed, landscape models account for terrain and fuel discontinuity (water bodies, highways etc.), while global fire models do not include this feature. Analysis, to which extent up-scaling from landscape level to a rather coarse grid cell of SEVER-FIRE should be done in the future.

5) Fire termination

Fire termination occurs with the onset of a significant rainfall event (more than 3 mm), causing weather danger to drop to zero. Close to cities, fire termination occurs after a delay dependent on distance to the city, as a proxy for human fire suppression. Fire suppression function (time to eliminate a fire) was constructed as a log-linear regression function from distance to the city, using fire duration statistics for Europe and Russia from EFFIS database (San Miguel-Ayanz et al., 2012). As a result, a single fire can continue in the model from one hour up to two days (see Eq. (11)):

$$\overline{duration} = 2 * (1 - \exp(-10^{-3} * dist), \qquad (11)$$

where *dist* is a distance (km) from a nearest city (area with $P > 400$ persons/km^2).

However, the limitation of maximum fire duration to two days was set due to range in the fire duration of EFFIS database, which covers mainly European domain. Globally this limitation may be not valid for remote high latitude areas, but even in these regions mathematical expectation of fire duration will be close to one day (see Korovin (1996)).

6) ***Estimation of fire effects***

The rate of spread is converted to an absolute value of average area burnt for one fire, using elliptic fire spread model (van Wagner, 1969) similarly to the Reg-FIRM approach (Venevsky et al., 2002), which is also adopted by majority of other global fire models.

Daily area burnt in the DGVM grid cell is calculated as Eq. (12):

$$aburnt(i) = N_{fire}(i) * S(i) + N_{fire}(i-1) * S(i), \quad (12)$$

where $N_{fire}(i)$ are number of fires, ignited in a day i, $N_{fire}(i-1)$ are number of fires continuing from previous day (if any do exist) and $S(i)$ is an area of spread for one fire, determined by vegetation and climate (see above). Equation (12) is a simplification of increase in areas of continuing fires as it does not account for a fact that growth of a next day fire starts from a perimeter of the previous day fire.

Daily burned area estimates are aggregated annually to estimate fire effects. Percentage of vegetation individuals killed depends on area burned and on resistance of each PFT to fires (Table 1), taken directly from the Glob-FIRM (Thonicke et al., 2001). The percentages are then converted to emissions, based on vegetation carbon content (dead PFT individuals are considered to be entirely burned), and daily redistributed following the profile of fire probability.

The model outlined above should be considered as an approach to design a global comprehensive process-oriented fire model based mainly on field observations and physically based assumptions. Still more analysis to be done for representation of fire processes within the model and calibration of parameters used in the model. For instance, study of Scott and Burgan (2005) indicated that moisture of extinction, used in SEVER-FIRE (see Table 1) may vary from 12% to 40%, for different fuel types, i.e. has a larger range than in our model. We plan to make sensitivity and optimization tests to improve the SEVER-FIRE model parameters and modifications of equations when necessary.

2.2 Data

2.2.1 Climate data

For this study, precipitation data from the National Centres for Environmental Prediction (NCEP climate data (minimum/maximum temperature, precipitation and convective precipitation, short-wave radiation and wind speed, http://www.cpc.ncep.noaa.gov/) were interpolated to 0.5 degree longitude/latitude spatial resolution for the period 1957 to 2006 (50 years). Daily wind speed is not well estimated in reanalysis approach (Kalnay et al., 1996), so it was averaged over the entire period and applied in simulation runs without inter-annual variability. The input soil texture data and CO_2 atmospheric concentration over the same period coincide with those of the LPJ-DGVM (Sitch et al., 2003). The model is run globally from bare soil state 15 times with the climate data for 50 (years and the CO_2 atmospheric concentration fixed for the year 1957 (spin-up period), in order to achieve equilibrium of soil carbon pools. From this equilibrium state, SEVER is forced by climate and atmospheric CO_2 for the period 1957- 2006 (transient period).

2.2.2 Socio-economic data

Distance from a city was pre-calculated from population density and the ratio of rural (urban) population. For this, areas where urban population density exceeds 400 persons/km^2 were considered as cities (UN definition of Human Settlements Program). Gridded population and rural (urban) ratio data sets for years 1940-2050, used by SEVER-FIRE were elaborated using UN Development Program estimates by major economic regions. Wealth index was calculated first for 600 cities around the globe (Svirejeva-Hopkins, personal communication) using approach of UN Human Settlement Program as a sum of six socio – economic components, each normalized to be ranged between 0 (minimum) and 5 (maximum). Components included GDP per capita, number of persons with high education, number of doctors, crime rate, access to clean potable water, air pollution level. Data for the cities was extrapolated for the entire land area using non-linear spline at a regular grid of DGVM. And Socio-economic data used in this study can be found at Code availability section.

2.3 Burned area and carbon emission validation data

GFED is a global 1º resolution database (van der Werf et al., 2006), which relies on three different active fire products calibrated to Moderate Resolution Imaging Spectrometer (MODIS) 500 meter burned area, for a temporal coverage spanning 1997-2006 (Giglio et al., 2006). Fire activity data from the Tropical Rainfall Measuring Mission (TRMM) – Visible and Infrared Scanner (VIRS (Giglio et al., 2003)) and European Remote Sensing Satellites (ERS) Along Track Scanning Radiometer (ATSR (Arino and Plummer, 2001)) sensors are used for the 1997-2001 period. Over 2001-2006, the calibration was based on active fires from MODIS (Giglio et al., 2006). Carbon emissions were then estimated based on those burned area estimates, with fuel loads calculated by the Carnegie-Ames-Stanford Approach (CASA) model (van der Werf et al., 2006).

The active fire to burned area calibration step and the use of three different sensors to build this dataset generate significant uncertainties on burned area estimates, which are considered to be about 50% at regional scales, although not quantified in the used version of GFED (van der Werf, personal communication). Used version of GFED also does not contain small fires. Emission uncertainties are consequently higher, taking into account their further dependence on the CASA model and on fuel loads and emission factor values.

2.4 Fire incidence, fire variability and carbon emission evaluation

We chose to focus primarily on burned area to evaluate the model at global scale, as this is a prerequisite to estimate carbon emissions. However, carbon emission being an essential aspect of biomass burning, its representation is briefly evaluated.

Fire incidence, seasonality, and inter-annual variability from SEVER are compared to GFED data over the 1997-2006 period. SEVER-DGVM considers grid cells to be 100% land or water. This required a few adjustments on both datasets (re-gridding of GFED data to SEVER lan-lon grid and overlay of two datasets), causing minor changes in the original GFED statistics (less than 3% for total global area burnt and global fire emissions). We consider burned fraction (BF) rather than burned areas, a latitudinal unbiased indicator of fire density given the use of a lat-lon grid.

Fire incidence is mostly dependent on three key factors, conceptualized by the fire triangle (Schoennagel et al., 2004): fuel availability, readiness of fuel to burn, and ignition source. SEVER spatial patterns of fire incidence are first compared to GFED, through the mean annual grid cell burned fraction (BF). BF drivers are then explored with a selection of relevant environmental variables, based on the fire triangle concept:

- Annual amount of precipitation, from the CPC merged Analysis of Precipitation (CMAP (Xie and Arkin, 1997)), provided by the NOAA/OAR/ESRL PSD, Boulder, Colorado, USA, (http://www.cdc.noaa.gov/).
- An indicator of dry season severity (DSS), which was constructed from precipitation (CMAP) and temperature data (NCEP/NCAR re-analysis project (Kalnay et al., 1996)). The indicator (Breckle, 2002), representing a rainfall deficit or a temperature excess, is computed as indicated by Fig. 4. Here we consider it as a rainfall deficit (unit: mm).
- Net Primary Productivity (NPP). Its influence on fires is estimated with NPP estimates from (Imhoff et al., 2004) and from SEVER.

- Land cover spatial distribution. SEVER-DGVM vegetation distribution and its impacts on BF patterns is evaluated with the Global Land Cover for the year 2000 (GLC2000 (Bartholomé and Belward, 2005)).

- Human rural and urban population density from the Global Demographic Data Collection (Vorosmarty et al., 2000), provided by the University of New Hampshire, EOS-WEBSTER Earth Science Information Partner (ESIP). An indicator of the rural predominance of the population was defined (Eq. (13)):

$$Rurality = \frac{rpop - upop}{rpop + upop}, \quad (13)$$

where $rpop$ and $upop$ being respectively the rural and urban population of the considered grid cell. *Rurality* varies between 1, fully rural, to -1, fully urban populations.

- Gross Domestic Product (GDP) gridded data (van Vuuren et al., 2007), provided by the Netherlands Environmental Assessment Agency.

We left aside wind speed, which significantly affects readiness of fuel to burn and fire spread, as an analyzed environmental variable, due to constrains put on it in the presented SEVER-FIRE simulations (see description of input data in Sect. 2.2). However, Lasslop et al. (2015) demonstrated that modification of rate of spread dependence by wind speed may influence sufficiently areas burnt, so we plan to explore wind speed as BF driver in the future.

We used CMAP precipitation data (extracted mainly from remote sensing data) in analysis to get more realistic relationship between fire regimes observed and precipitation. We, however, could not use CMAP precipitation as climate input for SEVER-DGVM due to too short period of observations (CMAP started from 1979) and used instead the NCEP reanalysis precipitation data which is longer and provide bigger ratio between lengths o transient and spin-up simulation periods in DGVM important for realistic description of vegetation and fires. Thus, discrepancies in relationships between fire and precipitations in our analysis for GFED and SEVER-FIRE cases can be to some extent explained by differences between NCEP and CMAP precipitation fields. These differences, however, have only regional character and do not change our general conclusion.

The relationship of chosen variables with fire incidence is not linear, and it involves multi-variable interactions. A more in-depth analysis of fire drivers would thus benefit from the use of multivariate statistics. We chose to avoid this level of complexity, since the most important conclusions are likely to be drawn from straightforward analysis, as a first evaluation of a global fire model. We thus analyze fire incidence through simple bi-dimensional plots.

Seasonality is evaluated via the fire season peak, i.e. the month with maximum fire activity for each grid cell. Inter-annual variability is compared to GFED both globally and regionally, to identify how the model performs on specific fire events and for different ecosystems. Again, in a similar way to fire incidence, fire inter-annual variability has been shown to depend on climatic and vegetation conditions. (Meyn et al., 2007) highlight three types of fire ecosystems, depending on their annual fire limitation by fuel amount, readiness of fuel to burn, or both, considering that the availability of ignition sources is relatively constant in time. Here, we further explore the climate impact on the readiness of fuel to burn, analyzing the implications of both fire season precipitation and fire season maximum temperature for fire inter-annual variability, along three ecosystem types (boreal, tropical humid, and dry/semi-dry). To extract those variables, the extent of the fire season in a grid cell was defined as the months with more than $1/12^{th}$ of the mean annual BF. Fuel availability, the second factor highlighted by Meyn et al. (2007), is also discussed.

3. Results

3.1 Fire incidence and emissions

Figure 5 shows the spatial distribution of the average annual BF for GFED and SEVER. GFED clearly depicts the most extensively burned continents, i.e. Africa and Australia. It also indicates high fire activity at the edges of the tropical forest, due to land clearing and pasture management, in Central and South America and South East Asia (Langner et al., 2007; Morton et al., 2006). Fire incidence is much lower in most temperate and boreal ecosystems, except for the north-western Iberian Peninsula and Kazakhstan, both regularly affected by fires. A few other regions display high BF values, for example eastern Siberia and Alaska. Note, however, that for ecosystems with a long fire return interval, as is the case in boreal regions, the statistics computed over 10 years are very sensitive to the occurrence of important fire events during that period, and it can not be considered representative of the long term regional fire regime. Eastern Siberia, for example, was highly affected by fires in 1998, boosting the 10 years average (Kajii et al., 2002; Le Page et al., 2008).

SEVER accurately reproduces some of the main spatial patterns of fire incidence, i.e. high BF values over Africa and Australia, very limited fire activity in the tropical evergreen forest and in most temperate and boreal regions. For a better emphasis of the discrepancies, Figure 6 illustrates the mismatch between GFED and SEVER through a normalized difference burned fraction index (NDBF) computed as Eq. (14):

$$NDBF = \frac{BF_{SEVER} - BF_{GFED}}{BF_{SEVER} + BF_{GFED}}, \quad (14)$$

Where BF_{SEVER} and BF_{GFED} are the annual fire incidence averaged over 1997-2006 from the model and the observations, respectively. $NDBF$ is constrained between -1 (large model under-estimation) and 1 (large model over-estimation). Finally, Figure 7 shows the gradient of three broad PFTs classes (Bare soil, Grass and Trees), as modelled by SEVER, and the regions of large over/under estimation of the actual tree cover percentage inferred from GLC2000. Those results and further comparison with GLC2000 clearly reveal the following patterns:

- Regions with low observed fire incidence and the presence of grass in the model display fire over-estimation, regardless of the GLC2000 landcover, and the more grass, the higher the over-estimation. This is the case for example in North America, India, South America and Papua New Guinea. The overestimation in these areas can be also caused by high fractional coverage of croplands, not included in SEVER-FIRE model.
- Regions with dominant tree cover, or with a large over-estimation of trees in the model, display under-estimation of fire incidence. This is the case in a large strip covering Kazakhstan and eastern Europe, and in most of South East Asia, for example.
- The model underestimates the very high fire incidence observed in sub-Saharan Africa.

Considering drivers of BF spatial distribution, Figure 8 illustrates the interactive influence of paired combinations of the previously described variables. In GFED, the most affected regions are clearly constrained by annual precipitation between 500 and 1500 mm/year and a dry season severity ranging from 150 to 500mm of rainfall deficit (Fig. 8: top). SEVER is less restrictive regarding this climatic limitation, but the general dependence patterns are similar to the observations. Concerning vegetation characteristics (Fig. 8: middle), fires affect ecosystems of all levels of NPP, although fire incidence is low at the extreme ends of the spectrum. Similar values of NPP and annual precipitation can be found in very different ecosystems, as in boreal and sub-tropical regions for example, with great differences in fire incidence, hence the low predictability of GFED BF by NPP and precipitation. SEVER also shows little constraining of the mean BF by the combination of those two variables. Finally, high fire incidence is biased towards rural regions with very low economic income (<600 US$/capita/year), as shown in Fig. 8: bottom, with the exception of Australia, the only wealthy country highly affected by fires. SEVER also shows this rural bias, but on average allows higher fire incidence in wealthy regions, including North America.

Finally, Figure 9 displays the mean annual carbon emissions for GFED and SEVER. Emissions are mainly dependent on fire incidence, the type and moisture content of the affected vegetation, and fire severity. In SEVER, dead PFTs individuals are entirely emitted to the atmosphere, while GFED takes into consideration combustion completeness. Consequently, the absolute level of emissions cannot be

compared, being much higher in SEVER, as expected. However, the spatial patterns reveal the importance of tropical savannas and forests in the global partitioning of carbon emissions in both GFED and SEVER, as well as a significant contribution from boreal regions. We are planning to correct SEVER for combustion completeness as well as for post-fire mortality processes.

3.2 Seasonality

Figure 10 shows the spatial patterns of the month with maximum fire activity for each grid cell, and the mismatch between GFED and SEVER. SEVER roughly reproduces the observed spatial patterns, with 73% of the grid cells with a mismatch lower than or equal to 2 months. Significant discrepancies occur in Sub-Saharan Africa, which peaks over March to June in the model, while GFED, along with other observation sources, indicate October to February (Barbosa et al., 1999a; Clerici et al., 2004; Dwyer et al., 2000b).

Sub-Saharan Africa is a major fire region (Dwyer et al., 2000c; Tansey et al., 2004), contributing to a large fraction of global fire activity from October to February, a period when most other regions experience little or no fire activity. As such, the inability of SEVER to reproduce fire seasonality in Sub-Saharan Africa is one of its major current limitations. Delayed fire season is also significant in Central North America and south-eastern Australia.

The fire seasonal cycle is partially driven by climate, but it can also be strongly influenced by human activities. Figure 11 illustrates the averaged profile of the fire season and the dry season over Sub-Saharan Africa, for those grid cells with a SEVER fire peak discrepancy larger than or equal to 4 months. For each of these cells, we computed the monthly fire season, centred the peak month on the x-axis, and then derived the corresponding monthly DSS profile. Once averaged over all grid cells, the fire and DSS profiles show the temporal connection between both variables. Figure 11 clearly indicates that in the grid cells considered, the fire season is shifted towards the early dry season in GFED, and towards the late dry season in SEVER.

In regions with lower use of fire as a management tool, as in boreal forests, the model performs much better and, along with the observations, tends to place the peak month in the middle or late dry season (not shown). The implication of these findings for model improvement are detailed in the discussion section.

3.3 Inter-annual variability

Figure 12 shows the grid cells correlation between annual BF timeseries from GFED and SEVER. Equatorial Asia, Mexico and a majority of boreal regions are in good agreement, along with part of South

America. As discussed later, those regions are characterised by their sensitivity to climate variability, especially to the El Niño of 1997/98 (Le Page et al., 2008). Poorest agreement is found in Africa, India, China, western Russia, south of the USA Great Lakes, and in parts of South America.

Inter-annual variability is further analyzed using a set of 13 regions, originally created for GFED analysis (Giglio et al., 2006) as represented in Fig. 13. Globally, and for each of those regions, Figure 14 shows the BF inter-annual anomalies from GFED and SEVER, along with the monthly distribution of fire activity as a further indicator of the timing of specific fire events, and of fire seasonality. The very poor agreement in the global plot was to be expected, given the discrepancies in mean spatial fire incidence (Fig. 5), resulting in different contributions from regions to the total fire anomalies. This is clearly revealed by the monthly plot, showing that total fire activity in December-February, peaking in GFED with the large contribution of sub-Saharan Africa, is very low in SEVER. Consequently, a given fire anomaly in Africa has a much bigger global impact in GFED than in SEVER.

Regional partitioning allows identifying and comparing specific fire events more easily, especially the ones driven by large scale climatic variability. The El Niño episode of 1997-1998 appears clearly in the BONA, CEAM, BOAS and EQAS regions in the observations, and is generally captured by the model with precise timing. Annually, the importance of those events is also reproduced for EQAS and BOAS, with respectively 1997 and 1998 being the peaking year in both GFED and SEVER. Generally, fire patterns in the other regions are not properly represented. The monthly resolution plots also give further insights into the regional scale seasonal cycle, which is generally very well reproduced, except for northern hemisphere Africa and Australia.

Figure 15 displays the dependence of fire anomalies on precipitation and temperature anomalies over the fire season, through their effect on soil and vegetation moisture status. Drought conditions are the main pre-requisite for fire occurrence within all vegetation types, although in low NPP ecosystems, low vegetation amount can be a limiting factor, resulting in a dependence of fire anomalies on growing season precipitation also (Holmgren et al., 2006; van der Werf et al., 2008). The relationship is first pictured globally (Fig. 15), showing that both precipitation and temperature anomalies are strong drivers, constraining positive fire anomalies almost exclusively to precipitation deficits, and towards positive temperature anomalies. This relationship is then analyzed in GFED for 3 types of ecosystems:

- Boreal ecosystems, a spatial aggregation of the BONA and BOAS regions. Boreal fires are shown to be strongly dependent on temperature, at a level comparable to precipitation.
- Tropical humid regions, selected within South America, Africa and Equatorial Asia, as the pixels with annual precipitation above 1500mm. Their fire anomalies are also strongly related to precipitation, while temperature is a weak driver.

- Semi-dry and dry African and Australian regions (annual precipitation below 500mm), which are characterised by high anthropogenic fire activity. For those regions, both fire season precipitation and temperature anomalies are poor predictors of fire anomalies.

Those patterns are well reproduced on a global scale, such that the patterns of dependence on both climatic variables are similar in the model and in observations (Fig. 15). In boreal/tropical humid ecosystems, SEVER shows the same trends towards more/less dependence on temperature, although not as neatly as in GFED. In the case of semi-dry and dry African and Australian regions, the model also shows a weaker dependence on precipitation and temperature, but stronger than in the observations.

4. Discussion

Perhaps one of the most important achievements of SEVER, as revealed by this study, is the realistic modelling of strong climate driven fire anomalies, such as the large biomass burning events resulting from El Niño-induced droughts in various regions of the world (Fig. 12 and Fig. 14). This climate induced variability is known to be considerable and has important consequences for atmospheric composition, the terrestrial carbon cycle, and biodiversity, as discussed in the Introduction. As such its accurate representation in DGVMs and ESMs is essential.

The in-depth analysis of this climatic influence highlights the variability of the precipitation/temperature dependence patterns (Fig. 15). Boreal regions are characterised by great annual amplitudes of precipitation and temperature. As such, both play an important role in the dynamics of soil and vegetation moisture status, through rainfall and evaporation, thus the strong fire dependence on both variables. In tropical humid regions, temperature variability is much lower, and only a major and prolonged precipitation deficit will result in fire prone conditions (van der Werf et al., 2008).

Finally, semi-dry and dry regions of Africa and Australia are characterised by a low dependence on both parameters. Those regions are under specific climatic conditions, characterised by a rather short and irregular wet season for vegetation growth, followed by a long dry season (Peel et al., 2007). Under those conditions, fuel availability, rather than its readiness to burn, limits the occurrence of fires (Meyn et al., 2007). Under low wet season precipitation, vegetation build-up may be too low to sustain a fire. Under high wet season precipitation, vegetation growth leads to less patchy vegetation, which will dry out over the following dry season, becoming highly susceptible to fires. This scheme is very specific of those hot dry and semi-dry regions dominated by annual herbaceous vegetation. In the case of middle to high productivity ecosystems with the presence of woody vegetation, the relationship is generally reversed: enhanced wet season precipitation leads to higher soil and vegetation moisture status, delaying desiccation over the dry season, thus reducing fire susceptibility. The contrast between those two distinct vegetation-

climate-fire relationships is most evident in Australia (Fig. 16). The SEVER vegetation scheme did not perform very well over Australia, and so the role of wet season precipitation is not properly represented (not shown).

At global scale, SEVER is shown to be fairly realistic regarding this temperature/precipitation dependence, which was to be expected since both variables are involved in the fire weather danger and fire spread calculations. However, the variability of the relationship along ecosystem types (boreal, tropical humid, semi-dry/dry), resulting from complex interactions between fire drivers, is not as straightforward to capture. The realistic results for such an interactive system suggests that the feedback mechanisms as defined in the SEVER-DGVM/SEVER-FIRE coupled scheme do reach a reasonable level of complexity and accuracy, especially in the case of boreal and tropical ecosystems.

The mean burned fraction (Fig. 5) is a more challenging feature for the model to replicate. Key associations represented in the fire triangle (Schoennagel et al., 2004) are, however, reproduced (Fig. 8), i.e. fire occurrence limitation by moisture in very humid ecosystems, or by low fuel amount in arid regions. Unfortunately, SEVER models potential - not actual - vegetation cover, hampering an in-depth diagnostic of the fire incidence estimates. However, grass/trees appear to be over/under sensitive to fires, with the exception of highest fire incidence regions (Africa, northern Australia), where SEVER underestimates fire activity, independent from vegetation cover (Fig. 6 and Fig. 7). The main PFT parameters controlling fire incidence are bulk density (fire ignition and spread, see Table 1), and flammability (fire danger index computation). Flammability takes the same value for all tree PFTs, and a distinct value for both C3 and C4 grasses together. As such, it may be a relevant factor to correct the over/under estimation observed in grass/trees. Of critical importance for fires are also three vegetation types not yet included in SEVER-DGVM: croplands and pasture (land management fires (Pyne, 2001)), savannas, and peatlands (modest land extent, but major carbon hotspot (Page et al., 2002; Turquety et al., 2007)).

It is also essential to improve our understanding of anthropogenic impacts on fire incidence. The initial assumptions of the model, with population and wealth status as the most important human proxies, are to be re-assessed carefully in regional studies, given the implication of other factors. Especially, the most evident cases of human induced increased or decreased fire activity are related to land use type and agricultural practices, more than to economic and social status. For example, Pfeiffer et al. (2013) divided population into three according to their dominating land use types: farmers, pastorals and hunter-gathers. Kaplan et al. (2016) showed that this division determined structure of areas burnt during Last Glacial Maximum. Thus, a simple timing function for rural population implemented into SEVER-DGVM may not work properly in Africa. Relating those ignitions to low wealth status, as done in SEVER, is certainly functional after a few adjustments, but seems less robust to other regions than an association of land use with timing of human pyrogenic activities and number of human ignitions. As an illustration, wealth status

is not well adapted to account for high fire incidence induced by humans in northern Australia (Russell-Smith et al., 2007). Additional proxies for human pyrogenic activities implemented in SEVER-FIRE could include deforestation activities (Zhan et al., 2002) and land use/landcover data (Thenkabail et al., 2006). Fire management factor should be added to the model in the regions where coordinated wildfire controlling program is in place (e.g. existence and actions of European Commissions Emergency Response Coordination Centre in Europe (https://ec.europa.eu/echo/what-we-do/civil-protection/forest-fires_en)).

Advantages of including relationship between land use and timing of pyrogenic activities in SEVER would possibly also extend to a better representation of fire seasonality. In sub-Saharan Africa for example, Figure 11 reveals that the fire season (October-February, Fig. 10) is shifted towards early months of the dry season, which mainly results from the use of fires for agricultural and land management practices (Clerici et al., 2004). For the whole southern hemisphere, however, human pyrogenic activity in SEVER is set to reach a maximum from March to May and September to November, which is not realistic in the case of sub-Saharan Africa, a major fire region. Timing of pyrogenic activities in sub-Saharan may be rather challenging as even implementation of land use in global fire model (Le Page et al., 2015) still brings 1 to 3 month delay in fire peak. Besides, it was demonstrated that religious affiliation modulates agricultural burning activities in the area (Pereira et al., 2015), which is completely off the view of global fire modelers at the time. It is seen that a set of regional case studies with an active use of available historical data is necessary to implement more realistic features of human pyrogenic activities in global fire models. Study and parameterization of fire duration in remote areas is necessary for improvement of area burnt calculation in these areas.

Description of lightning fires need also improvements, starting from estimation of number of lightning strikes effective for fire ignition. Despite lightning strike is considered to be to major extent a stochastic event, there is a visible room of better description of number of cloud-to-ground flashes based on recent findings of role of aerosols in electrification of thunder clouds (Stolz Douglas et al., 2015; Venevsky, 2014). In addition, sensitivity study for critical newly implemented features *timing* and *duration* and further formal optimization for parameters of SEVER-FIRE model using teaching subset of remote sensing data for observed areas burnt (Khvostikov et al., 2015; Rabin et al., 2015; Rabin et al., 2018) can further improve performance of the presented global fire model.

5. Conclusions

This paper analysis results from a DGVM which includes an interactive, dynamically-linked fire module. It reveals that the most important climate driven fire features are reproduced by the model, while the dependence on vegetation characteristics and, especially, human pyrogenic activities prevents the further

development of realistic estimates of fire incidence, and of regional to global inter-annual variability. Regional adjustments of global fire models based on analysis of both historical fire statistics/records and recent satellite observations are necessary for further understanding of global fire dynamics in past, present and future.

6 Code availability

SEVER-FIRE is presented in its 1.0 version, which is realised in FORTRAN language. It is open use scientific software. The source code of SEVER-FIRE and the socio-economic input data can be accessed freely from https://github.com/zjkwuchao/SEVER-FIRE-model.git

7 Author contributions

SV developed equations of the fire model. SV and CW worked on the code. YLP and JMCP suggested scheme of the model validation and made the validation. SV, YLP, JMCP, and CW equally contributed to writing of manuscript.

8 Competing interests

The authors declare no competing interests.

Acknowledgements

We thank Guido van der Werf for providing the GFED data and for helpful comments on the manuscript. This study is funded by the Marie Curie Research Training Network GREENCYCLES, contract number MRTN-CT-2004-512464 (www.greencycles.org), National Science Foundation of China (31570475), and Tsinghua University-Peter the Great St. Petersburg Polytechnic University Joint Scientific Research Fund (20173080026). We thank kind comments from the editors, Iain Colin Prentice, and two anonymous reviewers.

References

Albini, F. A.: Estimating wildfire behavior and effects, General Technical Report, INT-GTR-30,USDA Forest Service, Intermountain Forest and Range Experiment Station, Ogden Utah, 92pp., available online at:http://www.treesearch.fs.fed.us/pubs/29574, 1976.

Allen, D. J. and Pickering, K. E.: Evaluation of lightning flash rate parameterizations for use in a global chemical transport model, J. Geophys. Res. -Atmos., 107, ACH 15-11-ACH 15-21, doi:10.1029/2002jd002066, 2002.

Andela, N., Morton, D. C., Giglio, L., Paugam, R., Chen, Y., Hantson, S., van der Werf, G. R., and Randerson, J. T.: The Global Fire Atlas of individual fire size, duration, speed, and direction, Earth Syst. Sci. Data Discuss., 2018, 1-28, doi:10.5194/essd-2018-89, 2018.

Anderson, K.: A model to predict lightning-caused fire occurrences, Int. J. Wildland Fire, 11, 163-172, doi:10.1071/WF02001, 2002.

Andreae, M. O. and Merlet, P.: Emission of trace gases and aerosols from biomass burning, Global Biogeochem. Cy., 15, 955-966, doi:10.1029/2000GB001382, 2001.

Arino, O. and Plummer, S.: The Along Track Scanning Radiometer World Fire Altas – Detection of night-time fire activity. IGBP-DIS Working paper #23, Potsdam, Germany, available online at:http://www.kalteng.org/userfiles/htmleditor/ATSR-World-Fire%20Atlas1998a.pdf, 2001.

Arora, V. K. and Boer, G. J.: Fire as an interactive component of dynamic vegetation models, J. Geophys. Res. -Biogeo., 110, G02008, doi:10.1029/2005JG000042, 2005.

Bachelet, D., Lenihan, J., Daly, C., Neilson, R. P., Ojima, D. S., and Parton, W. J.: MC1: A Dynamic Vegetation Model for Estimating the Distribution of Vegetation and Associated Ecosystem Fluxes of Carbon, Nutrients, and Water, General Technical Report, PNW-GTR-508, USDA Forest Service, Pacific Northwest Research Station, Portland OR, 95pp., available online at:https://www.fs.usda.gov/treesearch/pubs/2923, 2001.

Barbosa, P. M., Gregoire, J. M., and Pereira, J. M. C.: An algorithm for extracting burned areas from time series of AVHRR GAC data applied at a continental scale, Remote Sens. Environ., 69, 253-263, doi: 10.1016/S0034-4257(99)00026-7, 1999a.

Barbosa, P. M., Stroppiana, D., Grégoire, J.-M., and Cardoso Pereira, J. M.: An assessment of vegetation fire in Africa (1981–1991): Burned areas, burned biomass, and atmospheric emissions, Global Biogeochem. Cy., 13, 933-950, doi:10.1029/1999GB900042, 1999b.

Bartholomé, E. and Belward, A. S.: GLC2000: a new approach to global land cover mapping from Earth observation data, Int. J. Remote Sens., 26, 1959-1977, doi:10.1080/01431160412331291297, 2005.

Baudena, M., Dekker, S. C., van Bodegom, P. M., Cuesta, B., Higgins, S. I., Lehsten, V., Reick, C. H., Rietkerk, M., Scheiter, S., Yin, Z., Zavala, M. A., and Brovkin, V.: Forests, savannas, and grasslands: bridging the knowledge gap between ecology and Dynamic Global Vegetation Models, Biogeosciences, 12, 1833-1848, doi: 10.5194/bg-12-1833-2015, 2015.

Benali, A., Mota, B., Carvalhais, N., Oom, D., Miller, L. M., Campagnolo, M. L., and Pereira, J. M. C.: Bimodal fire regimes unveil a global-scale anthropogenic fingerprint, Global Ecol. Biogeogr., 26, 799-811, doi:10.1111/geb.12586, 2017.

Bonan, G. B. and Doney, S. C.: Climate, ecosystems, and planetary futures: The challenge to predict life in Earth system models, Science, 359, doi:10.1126/science.aam8328, 2018.

Bond, W. J., Woodward, F. I., and Midgley, G. F.: The global distribution of ecosystems in a world without fire, New Phytol., 165, 525-537, doi:10.1111/j.1469-8137.2004.01252.x, 2005.

Bowman, D. M., Balch, J. K., Artaxo, P., Bond, W. J., Carlson, J. M., Cochrane, M. A., D'Antonio, C. M., Defries, R. S., Doyle, J. C., Harrison, S. P., Johnston, F. H., Keeley, J. E., Krawchuk, M. A., Kull, C. A., Marston, J. B., Moritz, M. A., Prentice, I. C., Roos, C. I., Scott, A. C., Swetnam, T. W., van der Werf, G. R., and Pyne, S. J.: Fire in the Earth system, Science, 324, 481-484, doi: 10.1126/science.1163886, 2009.

Breckle, S.-W.: Walter's Vegetation of the Earth. Springer, available online at: https://www.springer.com/us/book/9783540433156, 2002.

Cardoso Manoel, F., Nobre Carlos, A., Lapola David, M., Oyama Marcos, D., and Sampaio, G.: Long-term potential for fires in estimates of the occurrence of savannas in the tropics, Global Ecol. Biogeogr., 17, 222-235, doi:10.1111/j.1466-8238.2007.00356.x, 2007.

Cary, G. J., Keane, R. E., Gardner, R. H., Lavorel, S., Flannigan, M. D., Davies, I. D., Li, C., Lenihan, J. M., Rupp, T. S., and Mouillot, F.: Comparison of the Sensitivity of Landscape-fire-succession Models to Variation in Terrain, Fuel Pattern, Climate and Weather, Landscape Ecol., 21, 121-137, doi: 10.1007/s10980-005-7302-9, 2006.

Christian Hugh, J., Blakeslee Richard, J., Boccippio Dennis, J., Boeck William, L., Buechler Dennis, E., Driscoll Kevin, T., Goodman Steven, J., Hall John, M., Koshak William, J., Mach Douglas, M., and

Stewart Michael, F.: Global frequency and distribution of lightning as observed from space by the Optical Transient Detector, J. Geophys. Res. -Atmos., 108, ACL 4-1-ACL 4-15, doi: 10.1029/2002JD002347, 2003.

Clerici, N., Boschetti, L., Eva, H., and Gregoire, J. M.: Assessing vegetation fires activity and its drivers in West-Central Africa using MODIS and TRMM data, in: 2004 IEEE International Geoscience and Remote Sensing Symposium, Anchorage, AK, USA, 20–24 September 2004, doi: 10.1109/IGARSS.2004.1370768, 2004.

Crevoisier, C., Shevliakova, E., Gloor, M., Wirth, C., and Pacala, S.: Drivers of fire in the boreal forests: Data constrained design of a prognostic model of burned area for use in dynamic global vegetation models, J. Geophys. Res. -Atmos., 112, D24112, doi:10.1029/2006JD008372, 2007.

Duncan, B. N., Martin, R. V., Staudt, A. C., Yevich, R., and Logan, J. A.: Interannual and seasonal variability of biomass burning emissions constrained by satellite observations, J. Geophys. Res. -Atmos., 108, ACH 1-1-ACH 1-22, doi: 10.1029/2002JD002378, 2003.

Dwyer, E., Gregoire, J. M., and Pereira, J. M. C.: Climate and vegetation as driving factors in global fire activity. In: Biomass Burning and Its Inter-Relationships with the Climate System, Innes, J. L., Beniston, M., and Verstraete, M. M. (Eds.), Advances in Global Change Research, available online at: https://link.springer.com/chapter/10.1007/0-306-47959-1_10, 2000a.

Dwyer, E., Pereira, J. M. C., Gregoire, J. M., and DaCamara, C. C.: Characterization of the spatio-temporal patterns of global fire activity using satellite imagery for the period April 1992 to March 1993, Journal of Biogeogr., 27, 57-69, doi:10.1046/j.1365-2699.2000.00339.x, 2000b.

Dwyer, E., Pinnock, S., Gregoire, J. M., and Pereira, J. M. C.: Global spatial and temporal distribution of vegetation fire as determined from satellite observations, International Journal of Remote Sensing, 21, 1289-1302, 2000c.

Giglio, L., Kendall, J. D., and Mack, R.: A multi-year active fire dataset for the tropics derived from the TRMM VIRS, Int. J. Remote Sens., 24, 4505-4525, doi:10.1080/014311600210182, 2003.

Giglio, L., van der Werf, G. R., Randerson, J. T., Collatz, G. J., and Kasibhatla, P.: Global estimation of burned area using MODIS active fire observations, Atmos. Chem. Phys., 6, 957-974, doi:10.5194/acp-6-957-2006, 2006.

Hammill, K. A. and Bradstock, R. A.: Remote sensing of fire severity in the Blue Mountains: influence of vegetation type and inferring fire intensity, Int. J. Wildland Fire, 15, 213-226, doi:10.1071/WF05051, 2006.

Hantson, S., Arneth, A., Harrison, S. P., Kelley, D. I., Prentice, I. C., Rabin, S. S., Archibald, S., Mouillot, F., Arnold, S. R., Artaxo, P., Bachelet, D., Ciais, P., Forrest, M., Friedlingstein, P., Hickler, T., Kaplan, J. O., Kloster, S., Knorr, W., Lasslop, G., Li, F., Mangeon, S., Melton, J. R., Meyn, A., Sitch, S., Spessa, A., van der Werf, G. R., Voulgarakis, A., and Yue, C.: The status and challenge of global fire modelling, Biogeosciences, 13, 3359-3375, doi: 10.5194/bg-13-3359-2016, 2016.

Holmgren, M., Stapp, P., Dickman, C. R., Gracia, C., Grahams, S., Gutierrez, J. R., Hice, C., Jaksic, F., Kelt, D. A., Letnic, M., Lima, M., Lopez, B. C., Meserve, P. L., Milstead, W. B., Polis, G. A., Previtali, M. A., Michael, R., Sabate, S., and Squeo, F. A.: Extreme climatic events shape arid and semiarid ecosystems, Front. Ecol. Environ., 4, 87-95, doi:10.1890/1540-9295(2006)004[0087:ECESAA]2.0.CO;2, 2006.

Imhoff, M. L., Bounoua, L., Ricketts, T., Loucks, C., Harriss, R., and Lawrence, W. T.: Global patterns in human consumption of net primary production, Nature, 429, 870-873, doi:10.1038/nature02619, 2004.

Kajii, Y., Kato, S., Streets, D. G., Tsai, N. Y., Shvidenko, A., Nilsson, S., McCallum, I., Minko, N. P., Abushenko, N., Altyntsev, D., and Khodzer, T. V.: Boreal forest fires in Siberia in 1998: Estimation of area burned and emissions of pollutants by advanced very high resolution radiometer satellite data, J. Geophys. Res. -Atmos., 107, ACH 4-1-ACH 4-8, doi:10.1029/2001JD001078, 2002.

Kalnay, E., Kanamitsu, M., Kistler, R., Collins, W., Deaven, D., Gandin, L., Iredell, M., Saha, S., White, G., Woollen, J., Zhu, Y., Chelliah, M., Ebisuzaki, W., Higgins, W., Janowiak, J., Mo, K. C., Ropelewski, C., Wang, J., Leetmaa, A., Reynolds, R., Jenne, R., and Joseph, D.: The NCEP/NCAR 40-Year Reanalysis Project, Bull. Am. Meteorol. Soc., 77, 437-472, doi:10.1175/1520-0477(1996)077<0437:TNYRP>2.0.CO;2, 1996.

Kaplan, J. O., Pfeiffer, M., Kolen, J. C. A., and Davis, B. A. S.: Large Scale Anthropogenic Reduction of Forest Cover in Last Glacial Maximum Europe, PLoS One, 11, e0166726, doi: 10.1371/journal.pone.0166726, 2016.

Kelley, D. I. and Harrison, S. P.: Enhanced Australian carbon sink despite increased wildfire during the 21st century, Environ. Res. Lett., 9, 104015, doi: 10.1088/1748-9326/9/10/104015, 2014.

Khvostikov, S., Venevsky, S., and Bartalev, S.: Regional adaptation of a dynamic global vegetation model using a remote sensing data derived land cover map of Russia, Environ. Res. Lett., 10, 9, doi: 10.1088/1748-9326/10/12/125007, 2015.

Knorr, W., Kaminski, T., Arneth, A., and Weber, U.: Impact of human population density on fire frequency at the global scale, Biogeosciences, 11, 1085-1102, doi:10.5194/bg-11-1085-2014, 2014.

Korovin, G. N.: Analysis of the Distribution of Forest Fires in Russia. In: Fire in Ecosystems of Boreal Eurasia, Goldammer, J. G. and Furyaev, V. V. (Eds.), 48, Springer, Dordrecht, available online at: https://www.springer.com/la/book/9780792341376, 1996.

Langenfelds, R. L., Francey, R. J., Pak, B. C., Steele, L. P., Lloyd, J., Trudinger, C. M., and Allison, C. E.: Interannual growth rate variations of atmospheric CO2 and its delta C-13, H-2, CH4, and CO between 1992 and 1999 linked to biomass burning, Global Biogeochem. Cy., 16, 22, doi: 10.1029/2001GB001466, 2002.

Langner, A., Miettinen, J., and Siegert, F.: Land cover change 2002-2005 in Borneo and the role of fire derived from MODIS imagery, Glob. Change Biol., 13, 2329-2340, doi:10.1111/j.1365-2486.2007.01442.x, 2007.

Lasslop, G., Hantson, S., and Kloster, S.: Influence of wind speed on the global variability of burned fraction: a global fire model's perspective, Int. J. Wildland Fire, 24, 989-1000, doi: 10.1071/WF15052, 2015.

Lasslop, G., Thonicke, K., and Kloster, S.: SPITFIRE within the MPI Earth system model: Model development and evaluation, J. Adv. Model. Earth Syst., 6, 740-755, doi:10.1002/2013MS000284, 2014.

Latham, D. J. and Schlieter, J. A.: Ignition probabilities of wildland fuels based on simulated lightning discharges, Research Paper INT-411, USDA Forest Service, Intermountain Forest and Range Experiment Station, Ogden Utah, 16pp., available online at: https://www.frames.gov/catalog/8165, 1989.

Le Page, Y.: Anthropogenic and climatic control upon vegetation fires: new insights from satellite observations to assess current and future impacts, Ph.D. , Technical University of Lisbon, 143 pp., 2009.

Le Page, Y., Morton, D., Bond-Lamberty, B., Pereira, J. M. C., and Hurtt, G.: HESFIRE: a global fire model to explore the role of anthropogenic and weather drivers, Biogeosciences, 12, 887-903, doi: 10.5194/bg-12-887-2015, 2015.

Le Page, Y., Pereira, J. M. C., Trigo, R., da Camara, C., Oom, D., and Mota, B.: Global fire activity patterns (1996-2006) and climatic influence: an analysis using the World Fire Atlas, Atmos. Chem. Phys., 8, 1911-1924, doi: 10.5194/acp-8-1911-2008, 2008.

Le Quéré, C., Moriarty, R., Andrew, R. M., Peters, G. P., Ciais, P., Friedlingstein, P., Jones, S. D., Sitch, S., Tans, P., Arneth, A., Boden, T. A., Bopp, L., Bozec, Y., Canadell, J. G., Chini, L. P., Chevallier, F., Cosca, C. E., Harris, I., Hoppema, M., Houghton, R. A., House, J. I., Jain, A. K., Johannessen, T., Kato, E., Keeling, R. F., Kitidis, V., Klein Goldewijk, K., Koven, C., Landa, C. S., Landschützer, P., Lenton, A., Lima, I. D., Marland, G., Mathis, J. T., Metzl, N., Nojiri, Y., Olsen, A., Ono, T., Peng, S., Peters, W., Pfeil, B., Poulter, B., Raupach, M. R., Regnier, P., Rödenbeck, C., Saito, S., Salisbury, J. E., Schuster, U.,

Schwinger, J., Séférian, R., Segschneider, J., Steinhoff, T., Stocker, B. D., Sutton, A. J., Takahashi, T., Tilbrook, B., van der Werf, G. R., Viovy, N., Wang, Y. P., Wanninkhof, R., Wiltshire, A., and Zeng, N.: Global carbon budget 2014, Earth Syst. Sci. Data, 7, 47-85, doi: 10.5194/essd-7-47-2015, 2015.

Lehsten, V., Tansey, K., Balzter, H., Thonicke, K., Spessa, A., Weber, U., Smith, B., and Arneth, A.: Estimating carbon emissions from African wildfires, Biogeosciences, 6, 349-360, doi: 10.5194/bg-6-349-2009, 2009.

Lenihan, J. M. and Bachelet, D.: Historical Climate and Suppression Effects on Simulated Fire and Carbon Dynamics in the Conterminous United States. In: Global Vegetation Dynamics, John Wiley & Sons, Inc, doi: 10.1002/9781119011705.ch2, 2015.

Levine, J. S., Bobbe, T., Ray, N., Witt, R. G., and Singh, A.: Wildland fires and the environment: A Global Synthesis, UNEP/DEIAEW/TR.99-1, 1999.

Li, F., Levis, S., and Ward, D. S.: Quantifying the role of fire in the Earth system - Part 1: Improved global fire modeling in the Community Earth System Model (CESM1), Biogeosciences, 10, 2293-2314, doi: 10.5194/bg-10-2293-2013, 2013.

Melekhov, I.: Lesnaia promyshlennost'. Moskow, 1978.

Meyn, A., White, P. S., Buhk, C., and Jentsch, A.: Environmental drivers of large, infrequent wildfires: the emerging conceptual model, Prog. Phys. Geogr., 31, 287-312, doi: 10.1177/0309133307079365, 2007.

Morton, D. C., DeFries, R. S., Shimabukuro, Y. E., Anderson, L. O., Arai, E., Espirito-Santo, F. D., Freitas, R., and Morisette, J.: Cropland expansion changes deforestation dynamics in the southern Brazilian Amazon, P. Natl. Acad. Sci. USA, 103, 14637-14641, doi: 10.1073/pnas.0606377103, 2006.

Page, S. E., Siegert, F., Rieley, J. O., Boehm, H. D. V., Jaya, A., and Limin, S.: The amount of carbon released from peat and forest fires in Indonesia during 1997, Nature, 420, 61-65, doi: 10.1038/nature01131, 2002.

Pechony, O. and Shindell, D. T.: Fire parameterization on a global scale, J. Geophys. Res. -Atmos., 114, D16115, doi:10.1029/2009JD011927, 2009.

Peel, M. C., Finlayson, B. L., and McMahon, T. A.: Updated world map of the Koppen-Geiger climate classification, Hydrol. Earth Syst. Sci., 11, 1633-1644, doi:10.5194/hess-11-1633-2007, 2007.

Pereira, J. M. C., Oom, D., Pereira, P., Turkman, A. A., and Turkman, K. F.: Religious Affiliation Modulates Weekly Cycles of Cropland Burning in Sub-Saharan Africa, PLoS One, 10, e0139189, doi: 10.1371/journal.pone.0139189, 2015.

Pereira, J. M. C., Pereira, B. S., Barbosa, P., Stroppiana, D., Vasconcelos, M. J. P., and Gregoire, J. M.: Satellite monitoring of fire in the EXPRESSO study area during the 1996 dry season experiment: Active fires, burnt area, and atmospheric emissions, J. Geophys. Res. -Atmos., 104, 30701-30712, doi: 10.1029/1999JD900422, 1999.

Pfeiffer, M., Spessa, A., and Kaplan, J. O.: A model for global biomass burning in preindustrial time: LPJ-LMfire (v1.0), Geosci. Model Dev., 6, 643-685, doi: 10.5194/gmd-6-643-2013, 2013.

Prentice, I. C., Kelley, D. I., Foster, P. N., Friedlingstein, P., Harrison, S. P., and Bartlein, P. J.: Modeling fire and the terrestrial carbon balance, Global Biogeochem. Cy., 25, GB3005, doi: 10.1029/2010GB003906, 2011.

Pyne, S. J.: Fire: A brief history. University of Washington Press, available online at: http://www.environmentandsociety.org/mml/fire-brief-history, 2001.

Rabin, S. S., Magi, B. I., Shevliakova, E., and Pacala, S. W.: Quantifying regional, time-varying effects of cropland and pasture on vegetation fire, Biogeosciences, 12, 6591-6604, doi: 10.5194/bg-12-6591-2015. 2015.

Rabin, S. S., Melton, J. R., Lasslop, G., Bachelet, D., Forrest, M., Hantson, S., Kaplan, J. O., Li, F., Mangeon, S., Ward, D. S., Yue, C., Arora, V. K., Hickler, T., Kloster, S., Knorr, W., Nieradzik, L., Spessa,

A., Folberth, G. A., Sheehan, T., Voulgarakis, A., Kelley, D. I., Prentice, I. C., Sitch, S., Harrison, S., and Arneth, A.: The Fire Modeling Intercomparison Project (FireMIP), phase 1: experimental and analytical protocols with detailed model descriptions, Geosci. Model Dev., 10, 1175-1197, doi: 10.5194/gmd-10-1175-2017, 2017.

Rabin, S. S., Ward, D. S., Malyshev, S. L., Magi, B. I., Shevliakova, E., and Pacala, S. W.: A fire model with distinct crop, pasture, and non-agricultural burning: use of new data and a model-fitting algorithm for FINAL.1, Geosci. Model Dev., 11, 815-842, doi: 10.5194/gmd-11-815-2018, 2018.

Russell-Smith, J., Yates, C. P., Whitehead, P. J., Smith, R., Craig, R., Allan, G. E., Thackway, R., Frakes, I., Cridland, S., Meyer, M. C. P., and Gill, M.: Bushfires 'down under': patterns and implications of contemporary Australian landscape burning, Int. J. Wildland Fire, 16, 361-377, doi: 10.1071/WF07018, 2007.

San Miguel-Ayanz, J., Schulte, E., Schmuck, G., Camia, A., Strobl, P., Liberta, G., Giovando, C., Boca, R., Sedano, F., Kempeneers, P., McInerney, D., Withmore, C., Santos de Oliveira, S., Rodrigues, M., Durrant, T., Corti, P., Oehler, F., Vilar, L., and Amatulli, G.: Comprehensive Monitoring of Wildfires in Europe: The European Forest Fire Information System (EFFIS), in: Approaches to Managing Disaster – Assessing Hazards, Emergencies and Disaster Impacts, edited by: Tiefenbacher, J., InTech, 87–108, available online at: http://effis.jrc.ec.europa.eu/, 2012.

Schoennagel, T., Veblen, T. T., and Romme, W. H.: The interaction of fire, fuels, and climate across rocky mountain forests, Bioscience, 54, 661-676, doi:10.1641/0006-3568(2004)054[0661:TIOFFA]2.0.CO;2, 2004.

Scott, J.H., Brugan, R.E.: Standard Fire Behavior Fuel Models: A Comprehensive Set for Use with Rothermel's Surface Fire Spread Model, General Technical Report, RMRS-GTR-153, USDA Forest Service, Rocky Mountain Research Station, Fort Collins, CO, 72pp., available online at: https://www.fs.fed.us/rm/pubs_series/rmrs/gtr/rmrs_gtr153.pdf, 2005.

Sitch, S., Smith, B., Prentice, I. C., Arneth, A., Bondeau, A., Cramer, W., Kaplan, J. O., Levis, S., Lucht, W., Sykes, M. T., Thonicke, K., and Venevsky, S.: Evaluation of ecosystem dynamics, plant geography and terrestrial carbon cycling in the LPJ dynamic global vegetation model, Glob. Change Biol., 9, 161-185, doi: DOI 10.1046/j.1365-2486.2003.00569.x, 2003.

Stocks, B. J., Mason, J. A., Todd, J. B., Bosch, E. M., Wotton, B. M., Amiro, B. D., Flannigan, M. D., Hirsch, K. G., Logan, K. A., Martell, D. L., and Skinner, W. R.: Large forest fires in Canada, 1959–1997, J. Geophys. Res. -Atmos., 107, FFR 5-1-FFR 5-12, doi: 10.1029/2001JD000484, 2002.

Stolz Douglas, C., Rutledge Steven, A., and Pierce Jeffrey, R.: Simultaneous influences of thermodynamics and aerosols on deep convection and lightning in the tropics, J. Geophys. Res. -Atmos., 120, 6207-6231, doi: 10.1002/2014JD023033, 2015.

Tansey, K., Gregoire, J. M., Stroppiana, D., Sousa, A., Silva, J., Pereira, J. M. C., Boschetti, L., Maggi, M., Brivio, P. A., Fraser, R., Flasse, S., Ershov, D., Binaghi, E., Graetz, D., and Peduzzi, P.: Vegetation burning in the year 2000: Global burned area estimates from SPOT VEGETATION data, J. Geophys. Res. -Atmos., 109, 22, doi: 10.1029/2003JD003598, 2004.

Thenkabail, P. S., Biradar, C. M., Turral, H., Noojipady, P., Li, Y. J., Vithanage, J., Dheeravath, V., Velpuri, M., Schull, M., Cai, X. L., and Dutta, R.: An Irrigated Area Map of the World (1999) derived from Remote Sensing, Res., Rep., 105, Tech. rep., International Water Management Institute, Colombo, Sri Lanka, p.74, 2006.

Thonicke, K., Spessa, A., Prentice, I. C., Harrison, S. P., Dong, L., and Carmona-Moreno, C.: The influence of vegetation, fire spread and fire behaviour on biomass burning and trace gas emissions: results from a process-based model, Biogeosciences, 7, 1991-2011, doi: 10.5194/bg-7-1991-2010, 2010.

Thonicke, K., Venevsky, S., Sitch, S., and Cramer, W.: The role of fire disturbance for global vegetation dynamics: coupling fire into a Dynamic Global Vegetation Model, Globol Ecol. and Biogeogr., 10, 661-677, doi: DOI 10.1046/j.1466-822x.2001.00175.x, 2001.

Turner, D., Ostendorf, B., and Lewis, M.: An introduction to patterns of fire in arid and semi-arid Australia, 19982004, Rangeland J., 30, 95-107, doi: 10.1071/RJ07039, 2008.

Turquety, S., Logan, J. A., Jacob, D. J., Hudman, R. C., Leung, F. Y., Heald, C. L., Yantosca, R. M., Wu, S. L., Emmons, L. K., Edwards, D. P., and Sachse, G. W.: Inventory of boreal fire emissions for North America in 2004: Importance of peat burning and pyroconvective injection, J. Geophys. Res. -Atmos., 112, D12S03, doi:10.1029/2006JD007281, 2007.

Uman, M. A.: The Lightning Discharge, Academic Press, San Diego, CA, available online at: https://www.elsevier.com/books/the-lightning-discharge/uman/978-0-12-708350-6, 1987.

van der Werf, G. R., Randerson, J. T., Collatz, G. J., Giglio, L., Kasibhatla, P. S., Arellano, A. F., Olsen, S. C., and Kasischke, E. S.: Continental-scale partitioning of fire emissions during the 1997 to 2001 El Nino/La Nina period, Science, 303, 73-76, doi: 10.1126/science.1090753, 2004.

van der Werf, G. R., Randerson, J. T., Giglio, L., Collatz, G. J., Kasibhatla, P. S., and Arellano Jr, A. F.: Interannual variability in global biomass burning emissions from 1997 to 2004, Atmos. Chem. Phys., 6, 3423-3441, doi: 10.5194/acp-6-3423-2006, 2006.

van der Werf, G. R., Randerson, J. T., Giglio, L., Gobron, N., and Dolman, A. J.: Climate controls on the variability of fires in the tropics and subtropics, Global Biogeochem. Cy., 22, GB3028, doi: 10.1029/2007GB003122, 2008.

van Vuuren, D. P., Lucas, P. L., and Hilderink, H.: Downscaling drivers of global environmental change: Enabling use of global SRES scenarios at the national and grid levels, Global Environ. Change, 17, 114-130, doi: 10.1016/j.gloenvcha.2006.04.004, 2007.

Vazquez, A. and Moreno, J. M.: Patterns of Lightning-, and People-Caused Fires in Peninsular Spain, Int. J. Wildland Fire, 8, 103-115, doi: 10.1071/WF9980103, 1998.

Veblen, T. T., Kitzberger, T., and Donnegan, J.: Climatic and human influences on fire regimes in ponderosa pine forests in the Colorado Front Range, Ecol. Appl., 10, 1178-1195, doi: 10.1890/1051-0761(2000)010[1178:CAHIOF]2.0.CO;2, 2000.

Venevsky, S.: Importance of aerosols for annual lightning production at global scale, Atmos. Chem. Phys. Discuss., 2014, 4303-4325, doi: 10.5194/acpd-14-4303-2014, 2014.

Venevsky, S. and Maksyutov, S.: SEVER: A modification of the LPJ global dynamic vegetation model for daily time step and parallel computation, Environ. Model. Software, 22, 104-109, doi: 10.1016/j.envsoft.2006.02.002, 2007.

Venevsky, S., Thonicke, K., Sitch, S., and Cramer, W.: Simulating fire regimes in human-dominated ecosystems: Iberian Peninsula case study, Glob. Change Biol., 8, 984-998, doi:10.1046/j.1365-2486.2002.00528.x, 2002.

Vonnegut, B.: Some Facts and Speculations Concerning the Origin and Role of Thunderstorm Electricity. In: Severe Local Storms. Meteorological Monographs, American Meteorological Society, Boston, MA, available online at: https://link.springer.com/chapter/10.1007/978-1-940033-56-3_11, 1963.

Vorosmarty, C. J., Green, P., Salisbury, J., and Lammers, R. B.: Global water resources: Vulnerability from climate change acid population growth, Science, 289, 284-288, doi: 10.1126/science.289.5477.284, 2000.

Wierzchowski, J., Heathcott, M., and Flannigan, M. D.: Lightning and lightning fire, central cordillera, Canada, Int. J. Wildland Fire, 11, 41-51, doi: doi.org/10.1071/WF01048, 2002.

Wu, C., Venevsky, S., Sitch, S., Yang, Y., Wang, M. H., Wang, L., and Gao, Y.: Present-day and future contribution of climate and fires to vegetation composition in the boreal forest of China, Ecosphere, 8, e01917, doi: 10.1002/ecs2.1917, 2017.

Wu, M. C., Knorr, W., Thonicke, K., Schurgers, G., Camia, A., and Arneth, A.: Sensitivity of burned area in Europe to climate change, atmospheric CO2 levels, and demography: A comparison of two fire-vegetation models, J. Geophys.

Res.-Biogeo., 120, 2256-2272, doi: 10.1002/2015jg003036, 2015.

Xie, P. P. and Arkin, P. A.: Global precipitation: A 17-year monthly analysis based on gauge observations, satellite estimates, and numerical model outputs, Bull. Am. Meteorol. Soc., 78, 2539-2558, doi: 0.1175/1520-0477(1997)078<2539:GPAYMA>2.0.CO;2, 1997.

Yue, C., Ciais, P., Cadule, P., Thonicke, K., Archibald, S., Poulter, B., Hao, W. M., Hantson, S., Mouillot, F., Friedlingstein, P., Maignan, F., and Viovy, N.: Modelling the role of fires in the terrestrial carbon balance by incorporating SPITFIRE into the global vegetation model ORCHIDEE - Part 1: simulating historical global burned area and fire regimes, Geosci. Model Dev., 7, 2747-2767, doi: 10.5194/gmd-7-2747-2014, 2014.

Zhan, X., Sohlberg, R. A., Townshend, J. R. G., DiMiceli, C., Carroll, M. L., Eastman, J. C., Hansen, M. C., and DeFries, R. S.: Detection of land cover changes using MODIS 250 m data, Remote Sens. Environ., 83, 336-350, doi: 10.1016/S0034-4257(02)00081-0, 2002.

Table 1: 5 of the 35 parameters defined for each of the 10 SEVER PFTs.

PFTs	Moisture of extinction[1]	Fire resistance index[2]	Minimum coldest monthly mean T°C[3]	Maximum coldest monthly mean temperature[3]	Bulk density of fuel kg/m2
Tropical Broadleaved evergreen tree	0.3	0.12	15.5	∅	3
Tropical Broadleaved rain green tree	0.3	0.5	15.5	∅	2
Temperate Needleleaved evergreen tree	0.3	0.12	-2	22	10
Temperate Broadleaved evergreen tree	0.3	0.12	3	18.8	10
Temperate Broadleaved summer green tree	0.3	0.12	-17	15.5	10
Boreal Needleleaved evergreen tree	0.3	0.12	-32.5	-2	16
Boreal Needleleaved summer green tree	0.3	0.12	∅	-2	16
Boreal Broadleaved summer green tree	0.3	0.12	∅	-2	16
C3 perennial grass	0.2	1	∅	15.5	2
C4 perennial grass	0.2	1	15.5	∅	2

[1] *Involved in the computation of fire probability*

[2] *Involved in the computation of vegetation disturbance after a fire*

[3] *∅ indicates no limitation from the considered parameter*

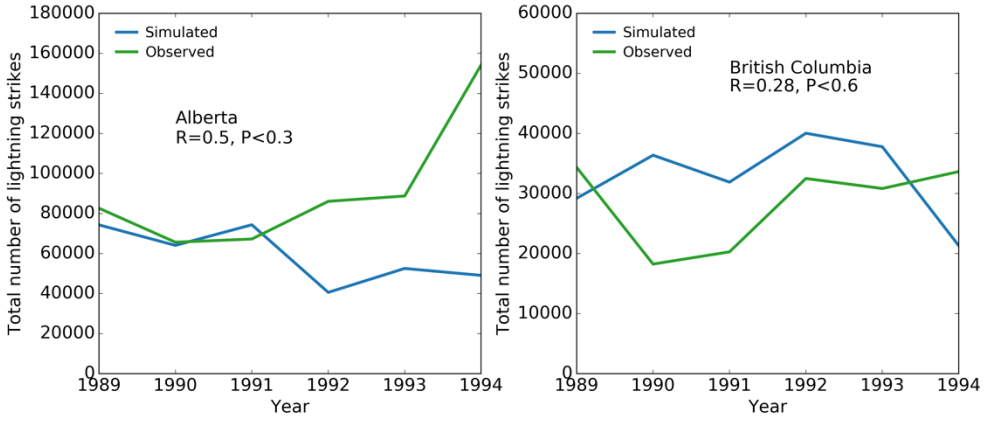

Figure 1. Observed and simulated number of lightning strikes in central cordillera of Canada. Left: in Alberta; Right: in British Columbia.

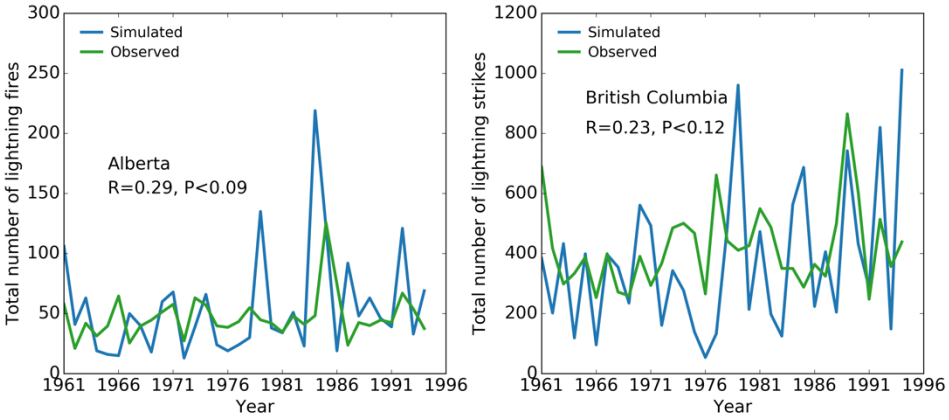

Figure 2. Total number of lightning fires observed (Wierzchowski et al., 2002) and simulated. Left: in Alberta; Right: in British Columbia.

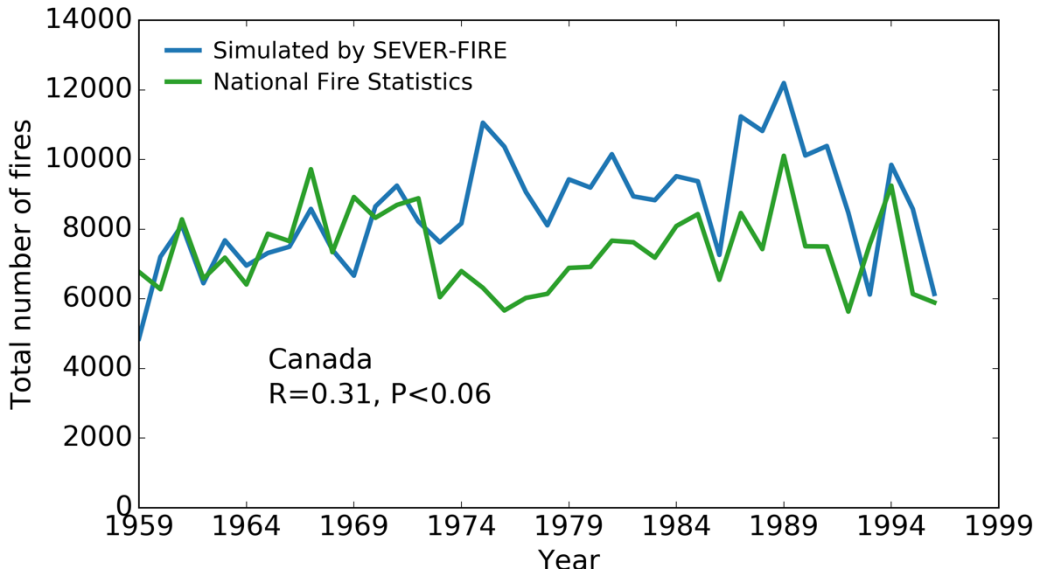

Figure 3. Registered and simulated number of fires in Canada.

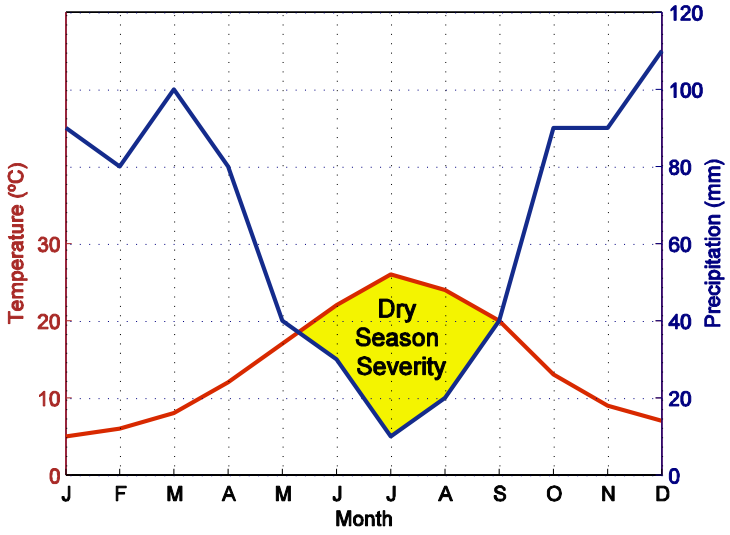

Figure 4: Definition of the dry season indicator on a climatic diagram as the yellow patch area. On the y-scales, 1ºC is equivalent to 2mm/year of precipitation, and Dry Season Severity (DSS) is computed as the area of the region where the temperature profile is above the precipitation profile.

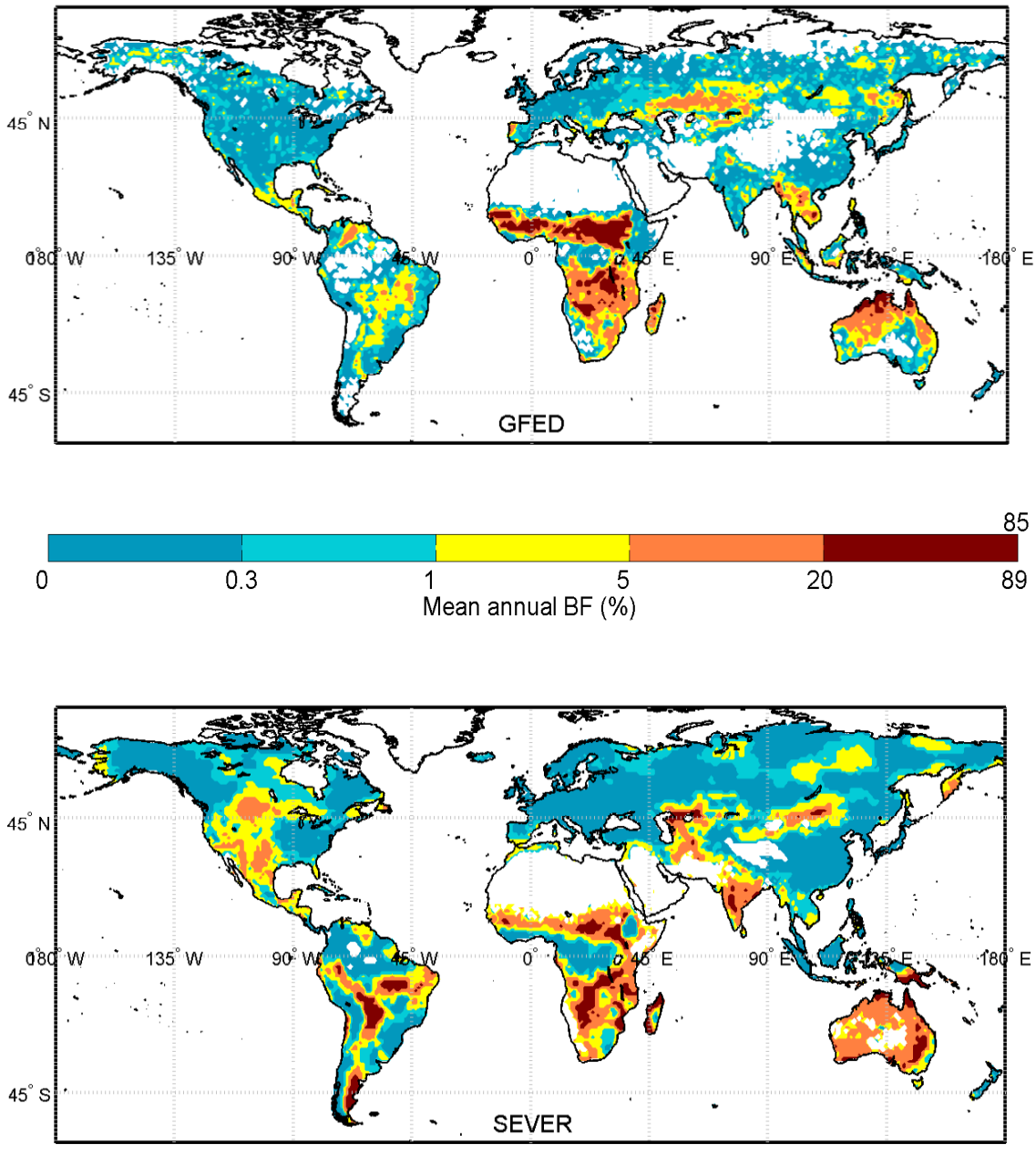

Figure 5. Mean Annual Burned Fraction (percentage) over 1997-2006. Top: GFED; Bottom, SEVER-FIRE.

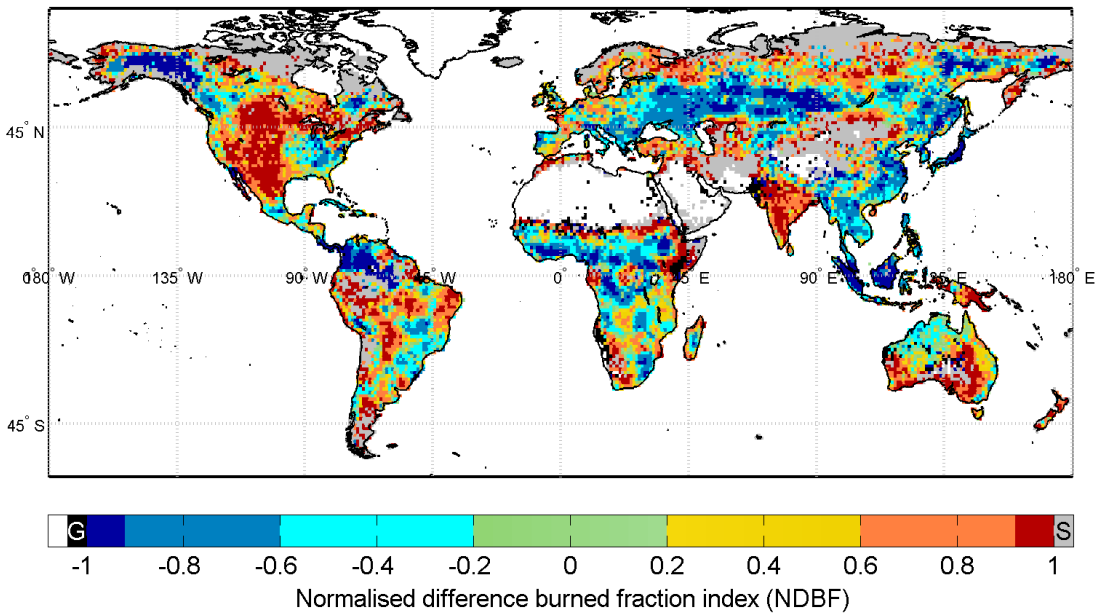

Figure 6. Discrepancies in the model outputs relative to GFED observation derived data, as represented by the normalised difference burned fraction index (see text). Black/grey colours represent grid cells where fires only occur in GFED/SEVER.

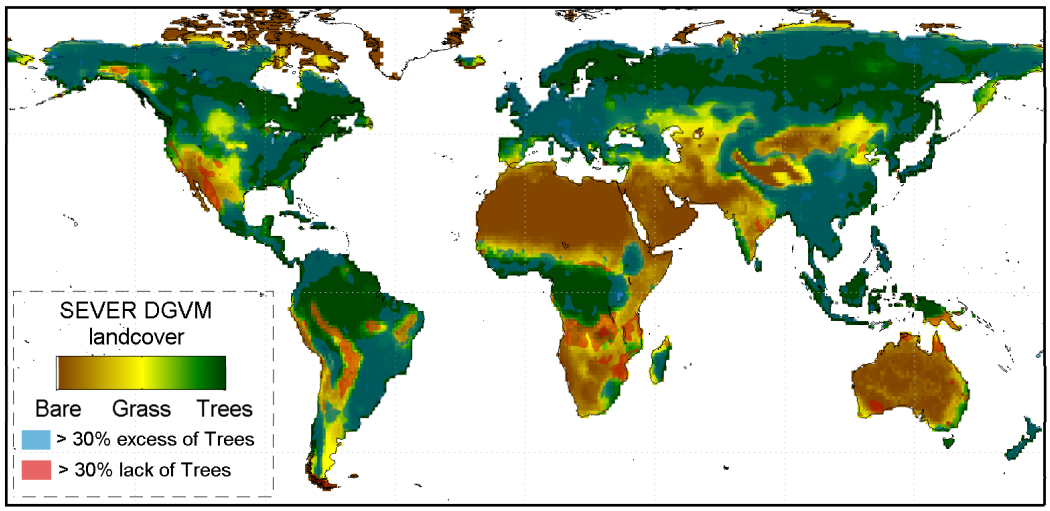

5

Figure 7. SEVER DGVM Land Cover distribution, grouped in 3 broad classes: Bare soil, Grass (C3 and C4) and Trees (all Tree PFTs, see Table 1).

10

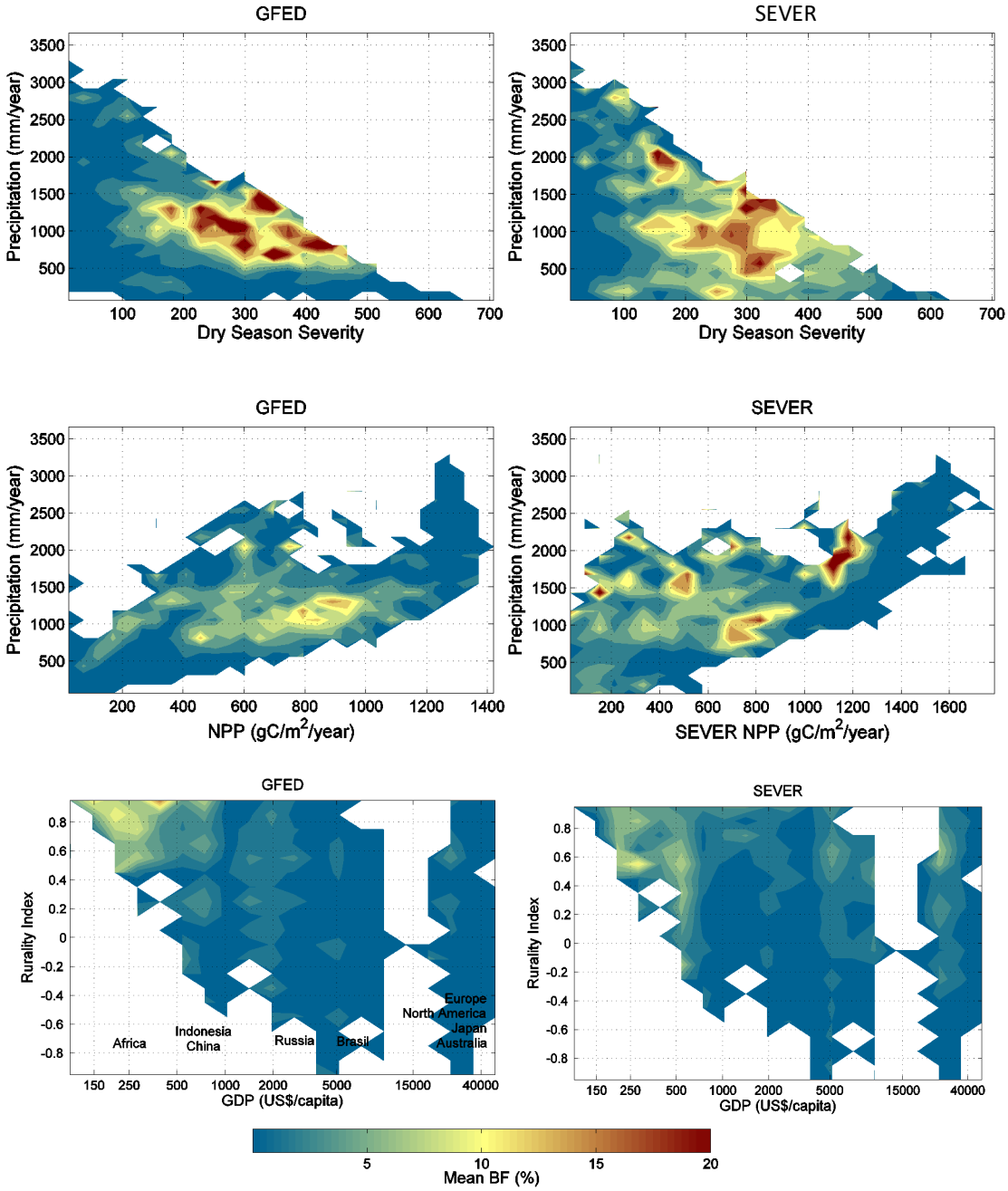

Figure 8. Mean Annual Burned Fraction over 1997-2006 (left: GFED; right: SEVER-FIRE) as a function of paired parameters. Top: Annual Precipitation and Dry season severity; Middle: Precipitation and NPP; Bottom: Rurality indicator and GDP.

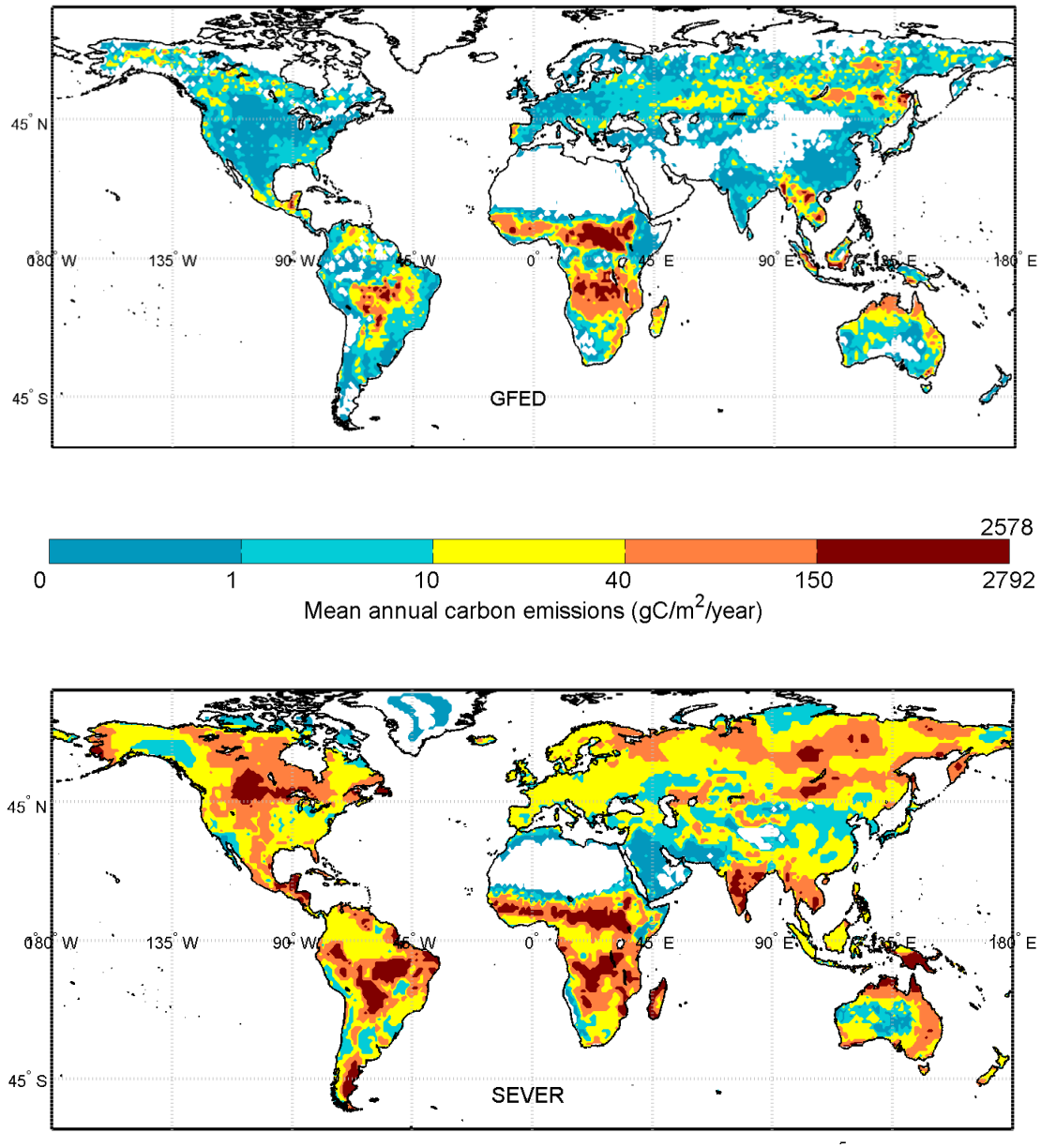

Figure 9. Mean Annual emissions (gC/m^2/year) over 1997-2006. Top: GFED; Bottom, SEVER-FIRE.

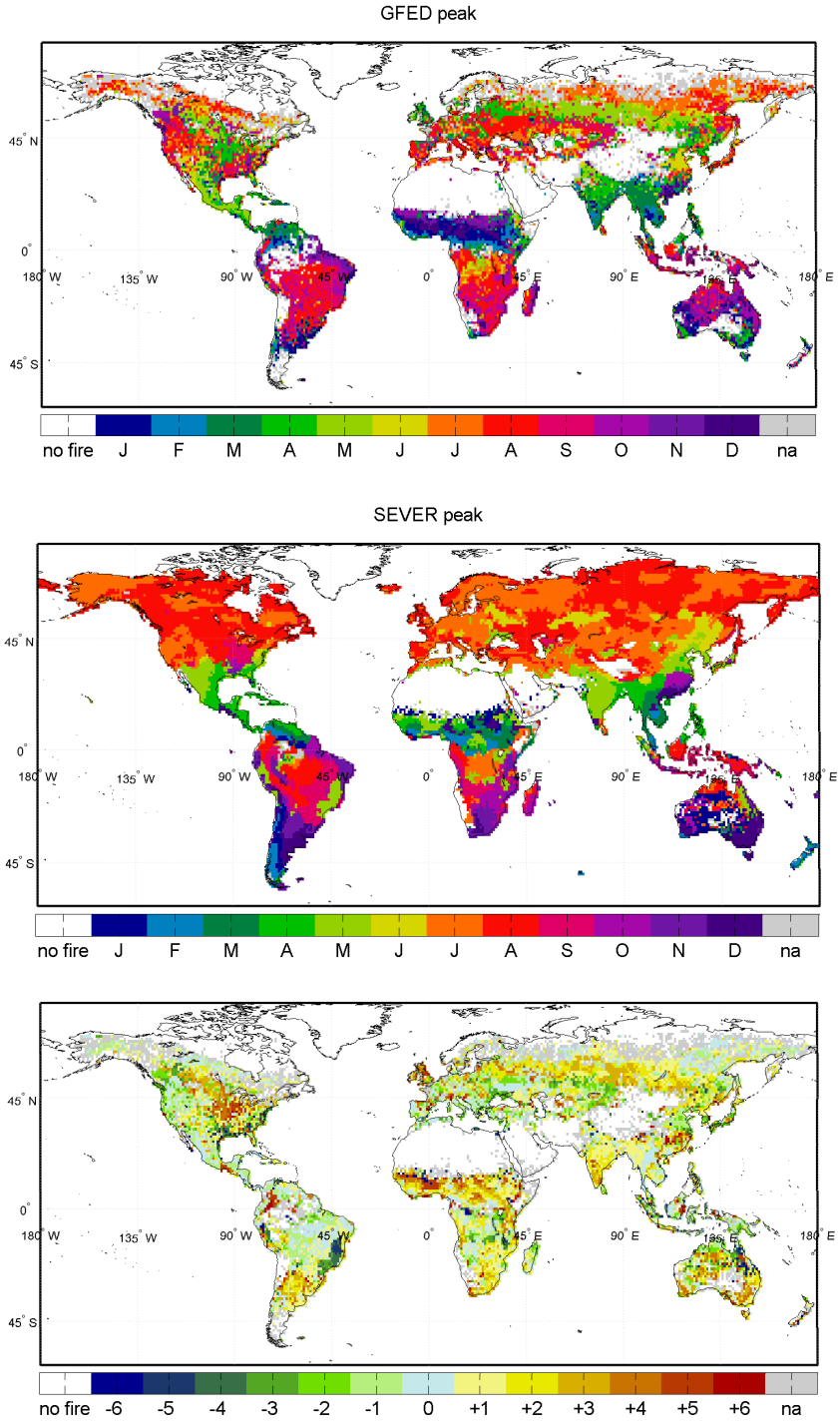

Figure 10. Top: Peak of the fire season in GFED; Middle: Peak of the fire season in SEVER; Bottom: relative mismatch between SEVER and GFED peaking month of the fire season.

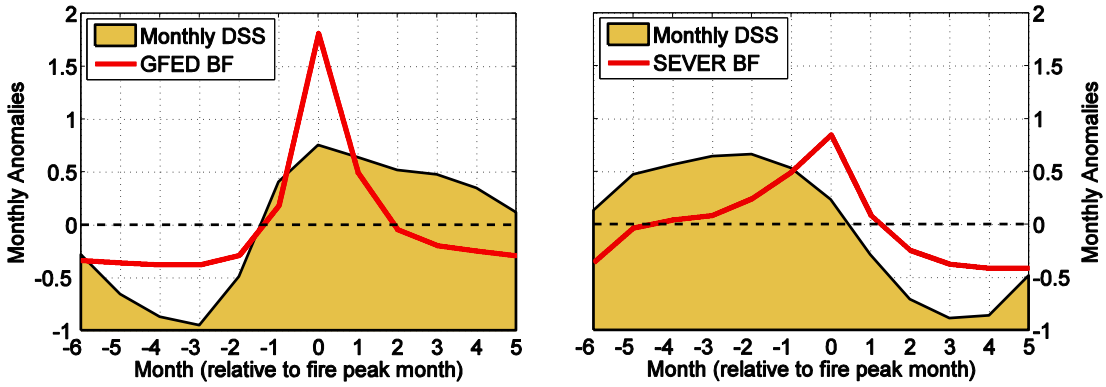

Figure 11. Averaged correspondence of fire season with dry season anomalies over regions of sub-Saharan Africa with a delay in peak month superior or equal to 4.

5

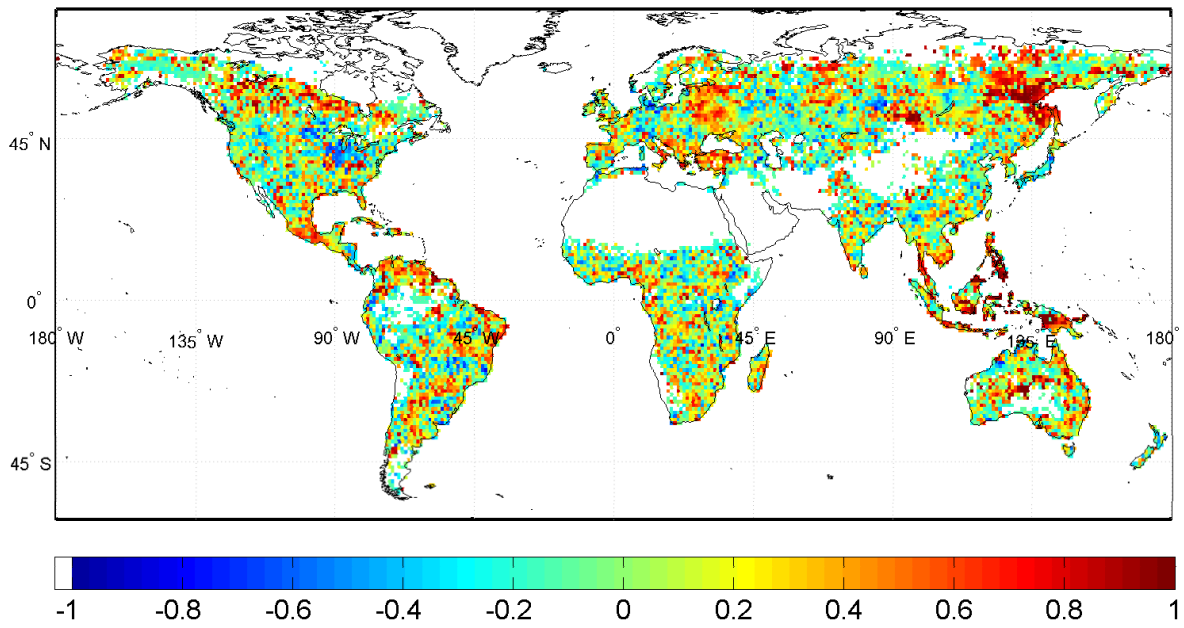

Figure 12. Correlation of annual BF from GFED and SEVER, over 1997-2006.

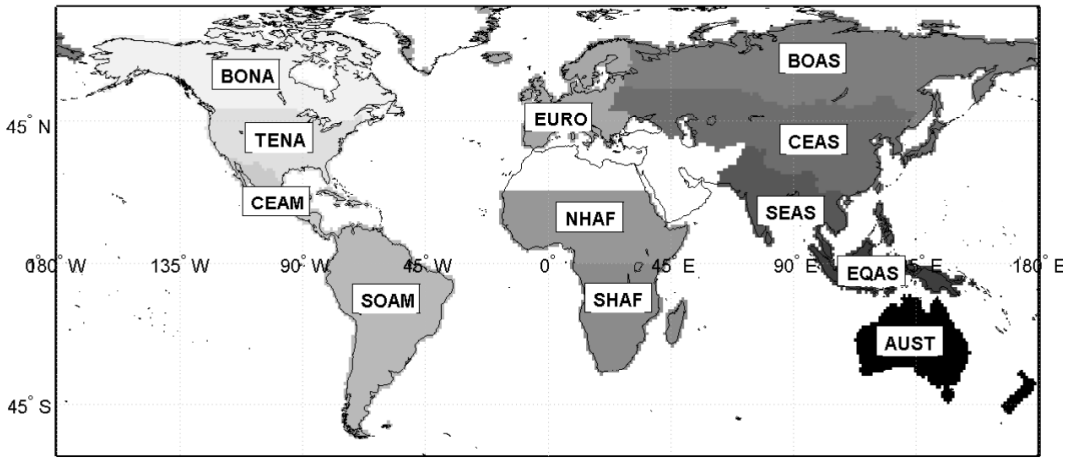

Figure 13. Regions used for inter-annual variability analysis. BONA: Boreal North America; TENA: Temperate North America ; CEAM: Central America ; SOAM: South America ; EURO: Europe ; NHAF: Northern Hemisphere Africa ; SHAF: Southern Hemisphere Africa ; BOAS: Boreal Asia ; CEAS: Central Asia ; SEAS: South East Asia ; EQAS: Equatorial Asia ; AUST: Australia.

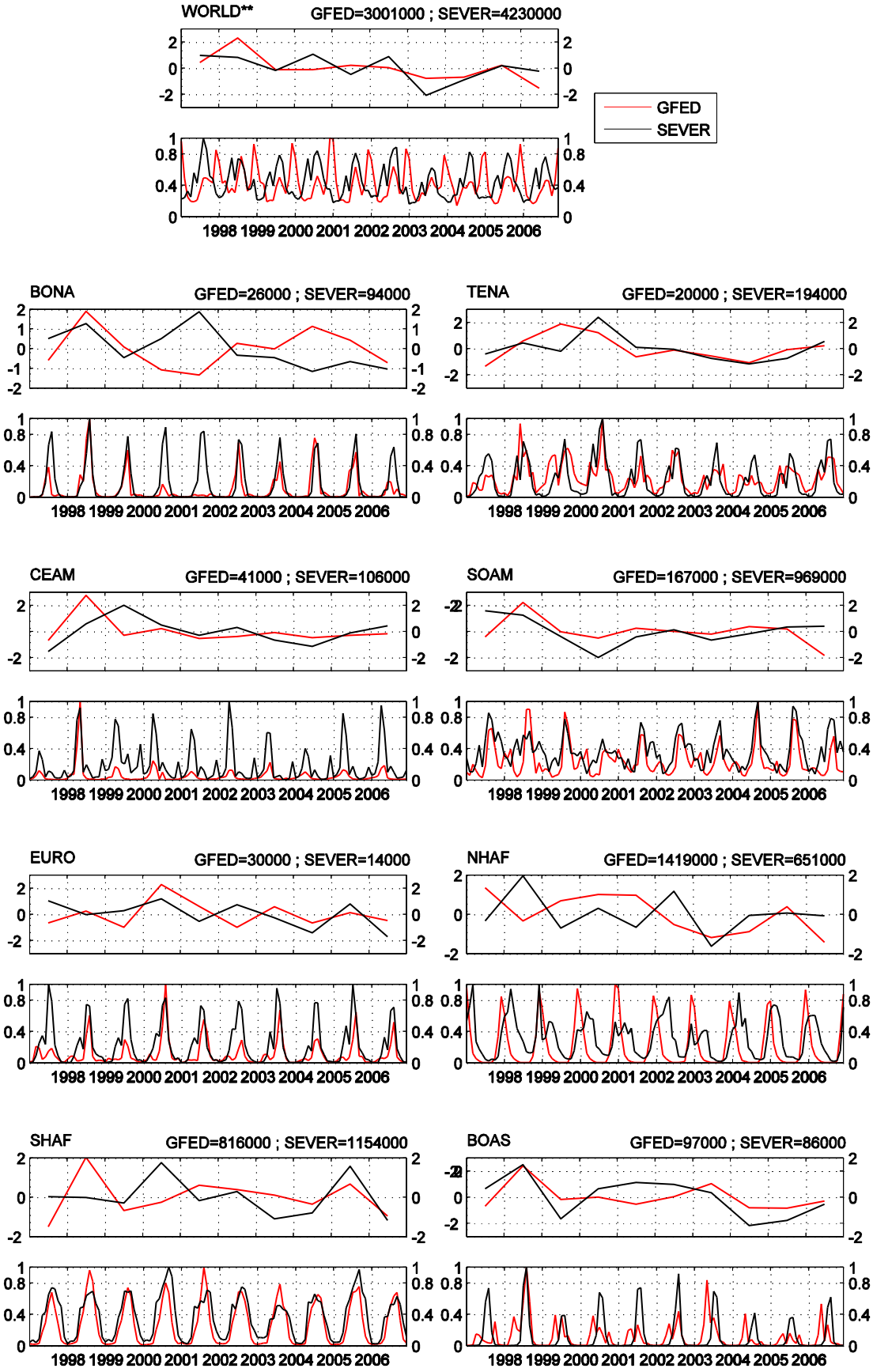
WORLD** GFED=3001000 ; SEVER=4230000
GFED
SEVER
BONA GFED=26000 ; SEVER=94000
TENA GFED=20000 ; SEVER=194000
CEAM GFED=41000 ; SEVER=106000
SOAM GFED=167000 ; SEVER=969000
EURO GFED=30000 ; SEVER=14000
NHAF GFED=1419000 ; SEVER=651000
SHAF GFED=816000 ; SEVER=1154000
BOAS GFED=97000 ; SEVER=86000
1998 1999 2000 2001 2002 2003 2004 2005 2006

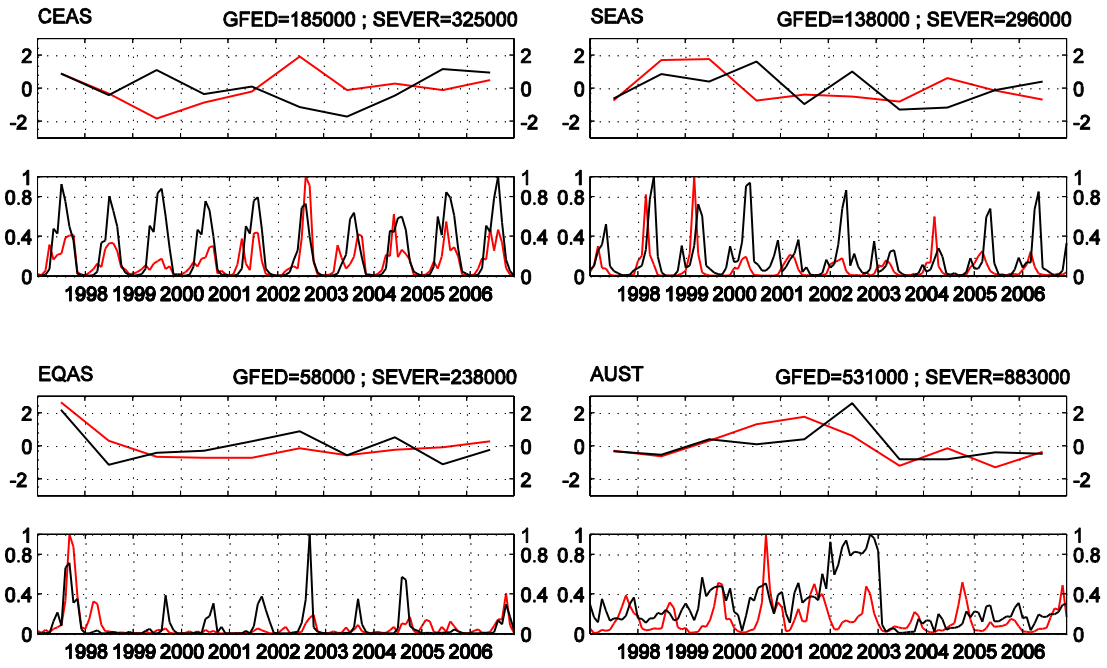

Figure 14. Regional comparison of fire variability over 1997-2006. For each region subplot: Top: annual Anomalies; Bottom: monthly time series constrained to [0 1]. The region name is indicated at the top left corner, the average fire incidence at the top right.

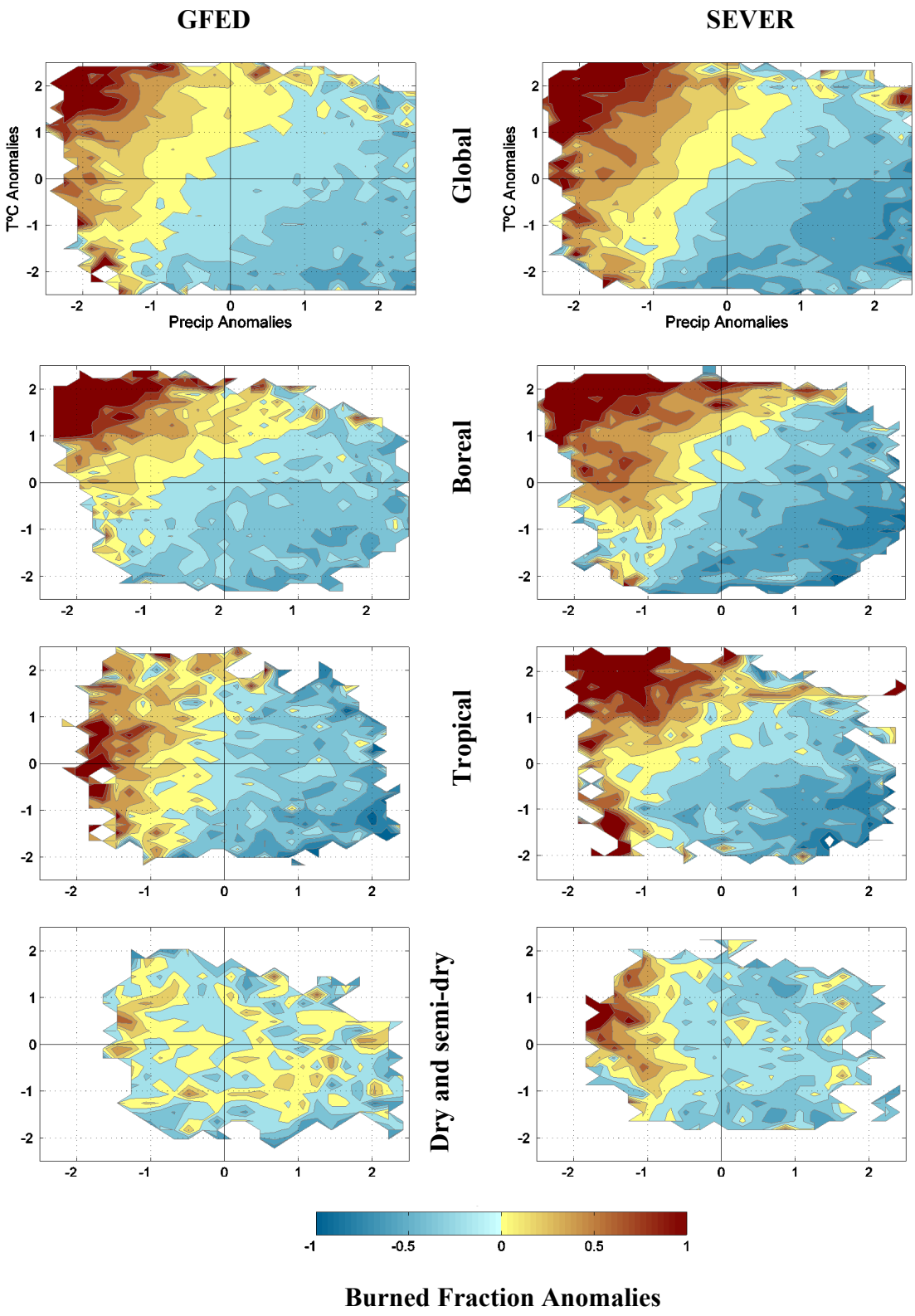

Figure 15: Dependence of fire anomalies to Temperature and Precipitation

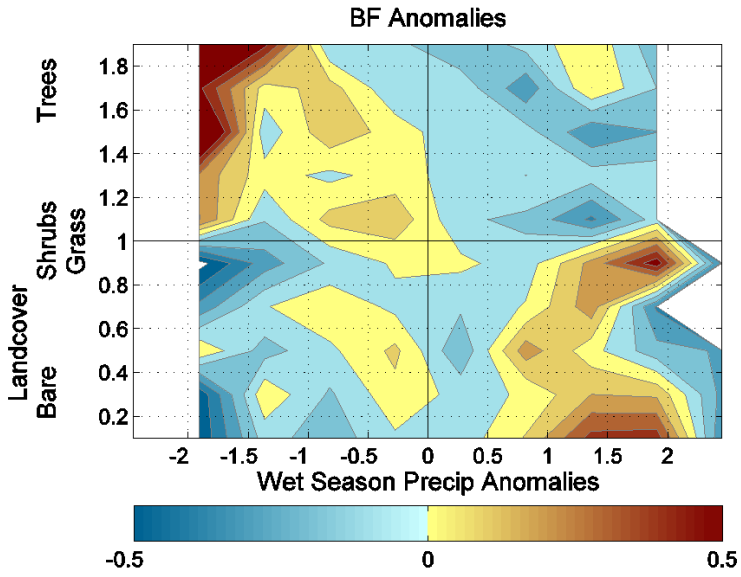

Figure 16: Dependence of fire anomalies to wet season precipitation and landcover type in Australia for GDED data